Master thesis

Improving the electrochemical protection of the linear part of gas pipelines

Vladislav Chernyshov

Date(08/07/2023)

Chair of Mining Engineering and Mineral Economics
Department Mineral Resources Engineering
Montanuniversitaet Leoben

A-8700 LEOBEN, Franz Josef Straße 18
Phone: +43 3842-402-2001
Fax: +43 3842-402-2002
bergbau@unileoben.ac.at

Declaration of Authorship

„I declare in lieu of oath that this thesis is entirely my own work except where otherwise indicated. The presence of quoted or paraphrased material has been clearly signaled and all sources have been referred. The thesis has not been submitted for a degree at any other institution and has not been published yet.”

Preface, Dedication, Acknowledgement

I acknowledge the Montanuniversitaet, Leoben, TU Bergakademie, Freiberg, Saint Petersburg mining university and the centre UNESCO for the great opportunity to learn and develop my knowledge in the field of Geoecology during the triple master's degree.

Abstract

This master's thesis addresses the issue of improving the efficiency of electrochemical protection of the main gas pipelines using the example of the section between 336-384 km of the main gas pipeline “Punga-Ukhta-Gryazovets III”.

The thesis studies the issues of using cathodic protection stations, reveals the main problems of gas main pipelines corrosion protection, conducts a scientific review of domestic and foreign scientific papers and the existing ways of solving these problems. The project also proposed a solution to the issue of optimizing the operation of electrochemical protection stations, develops mathematical models of protective potentials distribution at the “Punga-Ukhta-Gryazovets III” gas main section and verifies their reliability and adequacy by the methods of mathematical statistics. The project also calculates the parameters of cathodic protection units when using extended elastomeric anodic grounding conductors and justifies the replacement of steel anode grounding.

Zusammenfassung

Diese Masterarbeit befasst sich mit der Frage der Verbesserung der Effizienz des elektrochemischen Schutzes der Hauptgasleitungen am Beispiel des 336-384 km langen Abschnitts der Hauptgasleitung "Punga-Ukhta-Gryazovets III".

Die Dissertation untersucht die Problematik des Einsatzes von kathodischen Schutzstationen, zeigt die Hauptprobleme des Korrosionsschutzes von Gashauptleitungen auf, führt eine wissenschaftliche Auswertung in- und ausländischer wissenschaftlicher Arbeiten durch und untersucht die bestehenden Lösungsmöglichkeiten für diese Probleme. Im Rahmen des Projekts wurde auch eine Lösung für die Optimierung des Betriebs von elektrochemischen Schutzstationen vorgeschlagen, mathematische Modelle für die Verteilung der Schutzpotentiale im Gasleitungsabschnitt "Punga-Ukhta-Gryazovets III" entwickelt und ihre Zuverlässigkeit und Angemessenheit mit den Methoden der mathematischen Statistik überprüft. Im Rahmen des Projekts werden auch die Parameter der kathodischen Schutzanlagen bei Verwendung von verlängerten elastomeren anodischen Erdungsleitern berechnet und die Ersetzung der Stahlanodenerdung begründet.

Table of Contents

1. Introduction

Today, natural gas is technically, economically and environmentally superior to many other energy sources (Tcvetkov et al., 2020). As a result, natural gas has the potential to become the main fuel of the 21st century, replacing oil.

Currently, the natural gas industry is of strategic importance for the economic development of the Russian Federation (Litvinenko, 2020). Natural gas is the largest source of supplement to the state budget (about 50%); therefore, as the most important structural component of the development of national and regional productivity, it plays a huge role in the livelihood security of the population (Shaposhnikov et al., 2022; Tcvetkov et al., 2020)

In terms of transport services, gas transportation system of Russia is the largest in the world. Gas pipelines remain the safest way to transport gas over long distances and are therefore an important infrastructure system.

The reliable supply of gas to consumers is largely dependent on the operability of gas pipelines, most of which have been in operation for more than 20 years. With the development of oil and gas fields and the consequent expansion of pipeline systems, corrosion is becoming an increasingly important issue for the industry worldwide. The greatest threat to the integrity and reliable operation of mainline pipelines is the development of corrosion processes and the stress corrosion processes that occur under aggressive ground conditions (Dann and Maes, 2018).

Diagnosing the technical condition of steel pipelines is an important task because energy security and, in particular, the social and economic development of the country depend on the accident-free and reliable operation of the Russian fuel and energy complex, including the objects of gas trunk pipeline transport.

Pipeline failures and accidents can lead not only to significant energy losses, but also to serious environmental consequences and sometimes to fatal accidents (Belvederesi and Dann, 2017; Cheng, 2016; Ramírez-Camacho et al., 2017). Corrosion defects can have a negative impact on the serviceability and reliability of pipelines. Defect assessment is therefore essential for integrity management and failure prediction of corroded gas pipelines (Qin and Cheng, 2021). If the maximum

allowable operating pressure passes the reliability assessment, the corroded pipeline can continue to operate by determining the pipeline failure pressure.

When a pipeline reaches its design life, the failure rate typically increases due to various fracture processes that reduce the pressure resistance of the pipeline. In order to transport hydrocarbons safely and efficiently, it is important to improve the capability and accuracy of pipeline failure prediction (C. Wang et al., 2021a).

Protecting pipelines from corrosion processes is a key challenge for gas transmission companies. And the key to effective protection of pipeline facilities is to keep electrochemical protection (EPC) systems in optimal operating condition to reduce energy consumption, extend the life of EPC systems and reduce overhaul costs.

Current problems are the frequent failure of electrochemical protection system components and their power supplies, and the maintenance of overrun cathodic protection stations to cover areas with impaired drainage point protection potential. This leads to increased power costs and a reduction in the service life of the equipment and materials used in pipeline corrosion protection systems (Bornukovskaya et al., 2019). Determining the optimum mode of operation for CPS under such conditions can be complex, taking into account the different requirements for minimum and maximum potential values depending on the operating conditions and the presence of factors that contribute to the development of corrosion damage.

Currently, operating CPS operate in the protection potential maintenance regime, but the protective potential value is only monitored at the point of drainage, which does not take into account changes in the loading parameters of the CPS equipment along the gas pipeline, as well as changes in corrosive environmental parameters such as stray currents, soil resistivity and the mode of operation of neighbouring CPS. This in turn makes it difficult to select the optimum CPS operating mode that will allow for protection along the gas pipeline and long-term operation with minimal energy consumption.

Reducing the protection current not only means optimising power consumption, but also increasing the service life of one of the most expensive components of the CPS system, the anode grounding electrode, from which the current flows. A reduction

in current consumption by a factor of several during plant operation means that the frequency of overhauls can be reduced by a factor of several.

The aim of this work is to improve the efficiency of the CPS by using statistical methods to select the optimum parameters for its operation in order to ensure the reliable operation of the gas pipeline.

Objectives of this work:

- To study the basic normative documents on electrochemical protection of underground pipelines and cathodic protection stations;
- To analyse the existing methods of regulation of cathodic protection systems;
- To calculate the characteristics of electrochemical protection for gas pipelines using mathematical statistics; to use the results of the calculations to develop optimal regulatory recommendations for CPS;
- Demonstrating the replacement of anode grounding as a means of improving the efficiency of CPS.

2. Analysis of basic technology

The basic material used for making pipelines is steel, which is subjected to corrosive effects of the pipeline environment during operation.

The corrosion process depends on many factors, but always occurs in a corrosive system, which consists of the corrosive object (steel) and the corrosive medium (substance). The result is the loss of mechanical strength of the metal, i.e., corrosion damage.

The consequences of an accident are not only economic damage in the form of loss of transported hydrocarbon material, but also significant damage to the environment and the infrastructure of nearby communities. Maintaining a stable protection

potential on a pipeline can reduce the corrosion rate from more than one millimetre per year to 0.01-0.001 mm[1].

In addition, an important aspect of reliable and efficient corrosion protection of pipelines is the optimization of operating parameters of cathodic protection stations, as well as the selection of their components, in particular anode earthing switches.

The object of this study is electrochemical corrosion of main pipeline. The subject of the study is the method of electrochemical protection of section 336-384 km of the main gas pipeline "Punga-Ukhta-Gryazovets III" against corrosive effects of aggressive ground environment. The gas pipeline is laid in a swampy area with alternating sandy soils and peat bogs, and there is also the presence of organic inclusions.

According to the regulatory document[1], regardless of the method of laying the pipeline, corrosion protection must ensure its continuous operation during the entire operational life of the pipeline.

There are two types of corrosion protection for pipelines: active and passive. Active protection creates the conditions for protection against corrosion, whilst passive protection protects the pipeline from the environment.

Passive corrosion protection methods include various protective coatings. An insulating coating must be applied to prevent corrosion of metal pipelines, including main gas pipelines. Before coating, the pipe surface must be properly prepared by removing substances that cause rust: water, varnish residues, grease/oil stains and dirt. Varnishes, paints and powders are used to protect the outer surface of the pipe against corrosion. Insulating coatings must have low water and oxygen permeability, mechanical strength, high and stable adhesion to steel, resistance to cathodic cracking and good dielectric properties. The protective coating must also be resistant to mechanical damage and maintain its performance under various temperature conditions. Correct application of the insulation coating can significantly reduce the corrosion rate of a pipeline and prevent possible accidents and environmental damage.

---

[1] *SP 36.13330.2012 Main pipelines. Revised edition of SNiP 2.05.06-85 - Introduced 2013-07-01*, 2012

Active corrosion protection of pipelines is based on a combination of electrochemical reactions of electric current and the following ion exchange techniques:

- Anodic protection – the use of magnesium anodes that release magnesium ions in the presence of an electric current, thereby slowing down the destruction of the pipeline metal.
- Cathodic protection – the phenomenon of cathodic polarisation of the pipeline metal in the presence of direct current, whereby the pipeline becomes a low-potential cathode, thereby eliminating the possibility of corrosion propagation.
- Electric drainage protection is a series of measures to counteract stray currents by installing drainage protection, installing electrical shields, etc.

Irrespective of the corrosivity of the ground or terrain, the pipeline must be fully protected against corrosive effects by protective coatings and electrochemical protection. All contact connections in the electrochemical protection system and cable connections between pipeline and anode earth shall be at least as reliable and durable as the factory-approved insulation of the connecting cables. In a circuit consisting of anode earth, cathodic protection devices and pipework, only double polymer insulated cables shall be used for underground connection cable sections. Electrochemical protection of process communication cables for pipelines shall be designed in accordance with GOST 9.602-89.

A direct current generator is required to provide cathodic corrosion protection for the pipeline. The pipeline shall be connected to the “negative” pole of the generator. The “positive” pole is in turn connected to the anode earthing elements, which are buried in the same soil area. The distance from the anode elements to the pipeline must be fifty to one hundred metres. The wires connecting the pipeline to the generator must have a low resistance and be properly insulated. The current produced by the generator passes underground through the anodes and then into the pipeline, which acts as a cathode element. This process protects the pipeline from corrosion. The DC generator normally consists of a current rectifier fed from the mains via a transformer.

The anode protection consists of a magnesium block placed in the ground, which acts as an anode in the corrosion “cell” formed between the anode and the pipeline.

The current generated by the driving force of this “cell” travels along the following route: anode element, ground, pipe, wire, anode element. The low decomposition rate of the magnesium blocks ensures reliable anodic corrosion protection of the pipeline. This method is typically used for steel pipelines. In anodic protection, the magnesium block is placed in clay, which allows the anode elements to disperse evenly, also maintaining the necessary humidity and preventing the formation of a film that prevents magnesium decomposition.

All main gas pipelines in any method of installation, except above-ground, must be fully protected against corrosion by protective coatings and electrochemical protection, regardless of the corrosive activity of the ground[2].

Electrochemical protection consists in polarisation of metallic materials of the pipeline, thus avoiding short-circuiting on metallic surfaces. In general, the essence of electrochemical protection is to suppress anodic processes by artificial polarization (anodic or cathodic) of metal of protected structure from external source (Medvedeva et al., 2013).

Polarisation is the deviation of the electrode potential from its equilibrium value when current flows through the system. In polarisation the potential in the anodic region shifts towards positive values (anodic polarisation) and the potential in the cathodic region shifts towards negative values (cathodic polarisation). In order to obtain protective polarisation of the cathode, a protective potential from a direct current source can be applied, or an additional anode material with a more negative intrinsic potential than the cathode material can be used. Of the electrochemical elements occurring on the surface of buried metal structures, the main cause of cathodic polarisation is the limitation of access of oxygen, the main cathodic depolarising agent, to the surface where corrosion occurs (Medvedeva et al., 2013). The anodic polarisation is mainly due to the outflow of oxidised metal ions from the surface and the difficulty of their diffusion from this surface through the ground electrolyte.

The underground pipeline acts as a cathode; the electrolyte filling the pores in the ground, in turn, acts as an anode. The cathodic protection station, which generates

[2] *State Standard GOST R 51164-98 Steel pipe mains. General requirements for corrosion protection - Introduced 1999–07–01*, 1999, *STO Gazprom (Proprietary Standard) 9.2-002-2009 Protection against corrosion. Electrochemical protection against corrosion. Basic requirements - Introdused 2009-10-13*, 2010

the protective potential, is a direct current source. In this protection system, the negative pole of the current source is connected to the pipeline and the positive pole is connected to the anode earth electrode. An additional anode material with a more negative potential than the cathode material can be used to increase the protective effect. The length of the protected section of a single CPS depends on various factors, such as the corrosivity of the ground, the quality of the protective layer of the pipeline and the capacity of the protection station. The protective capacity prevents cathodic corrosion of the pipeline and ensures reliable operation without damage to the environment. At the same time, the anode, i.e., the anode ground, is intensively destroyed as a result of the activation of the anodic process.

The generally accepted standard for corrosion protection of pipelines is the protective total potential difference between pipe and ground and the polarisation potential defined as the potential difference in the “pipeline-ground” pair relative to the copper-sulphate reference electrode (Nikulin, 2015).

Figure 1 shows a model of the current distribution of the CPS. The potential φ_i at the drainage point of the cathodic protection station acts as a boundary condition and is set or changed as an input to optimise the CPS parameters (Skuridin et al., 2011). The pipeline section is divided into finite elements of length *ΔL*. The end elements are numbered *i-2, i-1, i, i+1, i+2* etc. The current j_i flows from the anode of the CPS to the pipeline and the current Ji flows through the protective zone of the pipe.

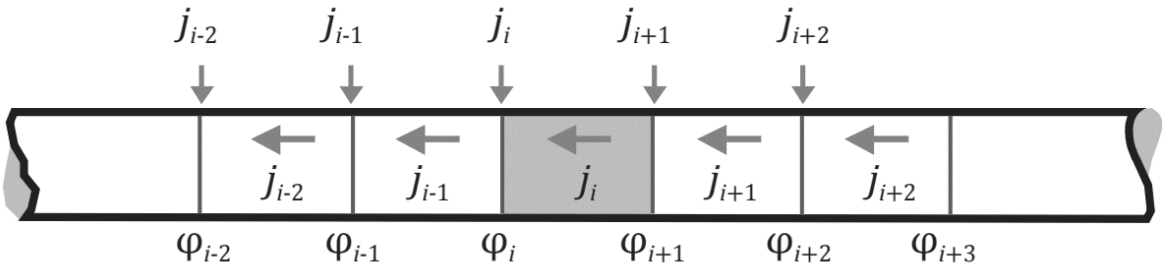

Figure 1: Scheme for a section of the CPS protection zone (Skuridin et al., 2011)

Experimental data show that the corrosion rate is minimal at an applied potential of -0.85 V (relative to the copper sulphate electrode). In the absence of factors significantly increasing soil erodibility, this will inhibit the corrosion process by 80-

85%. In Russia this potential is considered to be the minimum protective potential. In highly corrosive soils it is recommended to increase the standard (absolute value) to -0.95 V. The probability of electrochemical corrosion (ECC) increases significantly when the absolute level of the protective potential of the copper-sulphate electrode decreases (above -0.8 V). In this regard, the level of corrosion propagation through the electrochemical pathway is higher in the sections of the pipeline between cathodic protection stations, where the protective potential is generally lower (Lyubchik et al., 2011).

The potential for ECC strongly depends on the corrosive activity of the soil. In acidic soils (i.e., at pH < 5), the passivated magnetite film on the surface of pipes with broken insulation is either absent or rather friable, which increases the probability of ECC. At pH > 6, the passivated magnetite film is dense (especially in calcareous soils) and protects the pipe from ECC. Pipeline sections near steel mills, coal-fired power plants and livestock farms are particularly susceptible to electrochemical corrosion (Lyubchik et al., 2011).

Cathodic protection is achieved by maintaining a protective potential on the pipeline. This potential is measured with a high resistance voltmeter in relation to a copper sulphate saturated reference electrode located in the ground.

Electrochemical protection systems for main gas pipelines include cathodic protection devices, protector devices, drainage protection devices, measuring and diagnostic stations, remote control and remote control and corrosion monitoring facilities, as well as their power supply facilities. Depending on the specific operating conditions of the pipeline, the electrochemical protection system may include all or some of these elements.

The DC power supplies of CPS are subdivided into two groups. The first group consists of converter-rectifiers and the second group consists of generators such as wind turbines, thermoelectric generators, gas turbine driven electric generators, internal combustion engines, etc. On main gas pipelines, the most common type is a cathode station with a rectifier powered from AC mains. It is most appropriate to use this type of power source where AC power lines of 0.4, 6 and 10 kV are available. Two types of converters are most commonly used in the gas transmission system: thyristor converters (where the protective current is regulated by the electronic phase control of the thyristor) and inverter converters (the essence of

which is to increase efficiency by double conversion of energy and reduction of losses on the high-frequency transformer).

The conditions for the mandatory application of electrochemical protection are detailed in SNIP 20506-85.

Anode earthing is one of the main components of the cathodic protection device, and the effectiveness of the whole electrochemical protection system depends largely on its reliable operation.

Anode grounding, in terms of design and depth, can be divided into the following types[3]:

- Subsoil earthing installed in the soil up to 10 m below the ground surface with horizontal, vertical or combined arrangement of electrodes.
- Deep earth grounding, installed in specially drilled boreholes, e.g., pile anode grounding and deep anode grounding using casing as anode grounding, with the working part reaching the surface, and pile earth grounding with reaching the surface.
- Extended earthing, usually laid along the structure to be protected (decommissioned underground steel structures can be used as extended horizontal anode grounding).

Anode grounding electrode is the main element of cathodic protection system for underground gas pipelines, which is in direct contact with the corrosive medium and is designed for distribution and flow of protective current into the corrosive medium.

In general, the construction of anode earth electrodes consists of the following main elements:

- the electrode (i.e., the working element);
- connecting conductive wire;
- contact node.

For deep anode ground electrodes, the following additional structural elements are also necessary:

[3] *RD 153-39.4-039-99 Standards for the design of electrochemical protection of main pipelines and oilfield sites*, 1999

- gas outlet tube;
- fastening assembly for bundling.

The design of the extended anode earth electrode provides for uniform wear of the working element material over its entire surface.

As a result of long-term operation of the main gas pipelines, defects in the protective coatings arise, which contributes to the formation of local areas of protection failure. The following methods are used to restore the protective capacity:

- Increasing the number of CPS in the pipeline section;
- Applying of a new insulation coating of the pipeline;
- Changing the type of anode grounding used;
- Changing the operation modes of auxiliary protection devices by setting optimum operating parameters.

Due to the fact that most of these methods require higher material investments, the last two methods are the most preferable. Increase of service life of main gas pipelines is possible due to optimization of electrochemical protection parameters and increasing of effectiveness of pipeline corrosion protection level control.

For optimization of CPS performance, it is necessary to reveal dependence of pipeline protection potential value on CPS output parameters. For experimental definition of this dependence by existing methods it is required to find coefficients of influence of each CPS on the total potential difference. And for the latter, in its turn, it is necessary to define the stationary potential, which is equal to the intrinsic potential of the gas pipeline metal at switching-off all CPS influencing on it, and also at pipeline depolarization. This is rather difficult to achieve on an operating pipeline with a good insulation coating. Accordingly, an alternative solution for determining dependence of protective potential distribution of the pipeline on the output parameters, in particular, on the value of current. In this paper we take as a base the solution of the described task suggested by the author (Nikulin et al., 2014; Nikulin, 2015) – using the introduced parameter of the external potential difference instead of using the own potential of the CPS system.

Besides the above-described way of optimisation of CPS operation in the process of pipeline corrosion protection, another effective method is optimal selection of anode earth electrodes suitable for particular conditions of pipeline operation. In

particular, this paper proposes replacement of deep anode earth electrodes with extended anode earth electrodes using elastomeric electrodes.

Series of elastomeric anode ground electrodes for electrochemical protection of underground pipelines is one of the representative examples of production organisation that has fundamentally changed the principles of technical processes in electrochemical protection from designing to operation. The main technical characteristics inherent in this type of electrodes include: possibility of creation and control of electric grounding field in electrochemical protection system, creation of necessary protective potential at the protected object, regardless of its size and construction, taking into account conductivity of corrosive medium, other consumer qualities, providing their application in electrochemical protection systems, minimum requirements for transportation, simplicity and convenience of installation, reliability and maintainability.

3. Research part

3.1 Literature review

Due to the effects of corrosion, oil and gas pipelines are subject to wear, leaks, fractures and failures. Optimally selected protection methods can prevent corrosion of steel pipelines, especially in unfavourable conditions and in aggressive soils. Properly selected and timely applied corrosion protection methods can reduce wear and tear on gas pipelines, extend their service life and qualitatively improve the transport of hydrocarbons.

It is well known that the main factors affecting the efficiency of protection against corrosion cracking in underground pipelines are: the corrosion activity on the ground, the state of the anticorrosion protection layer of the protected object, the parameters of the protected object itself and the characteristics of the means of protection.

Methods of preventing external corrosion of pipelines are divided into passive, active and mixed protection methods. Passive methods include coatings, linings, barriers, electrical insulation, inhibitors, etc. While active methods of corrosion

protection include the use of sacrificial (electrochemical) anodes and pulsed current cathodic protection. Active and passive methods are often combined to provide a more comprehensive corrosion protection system against newly discovered causes of corrosion or coating degradation (Farh et al., 2023).

Although corrosion damage to metallic pipelines is a common and frequent problem, it remains uncontrollable even with the use of advanced corrosion protection techniques. It is therefore important to understand the factors that contribute to corrosion in metallic pipelines (Farh et al., 2023).

Soil resistivity, the acidity of the medium (i.e. pH), humidity, temperature, redox potential, organic content of the soil, mineral composition, the presence of bacteria and soil type are all external factors that contribute to accelerated pipeline corrosion (Wasim et al., 2018). Each factor has a definite effect. For example, soil resistivity decreases with increasing water content and chloride concentration. Soil properties, mineral and chemical composition are considered to be the most common external corrosion factors at 12%, with coating damage and degradation considered to be the third most common external corrosion factor at 10% (Wasim et al., 2018).

Stray currents caused by energy infrastructure (trams, railways, AC lines) are considered to be the fourth most common external corrosion factor, accounting for 4%. Other factors, such as biochemical or bacterial activity, hydrogen embrittlement and stress corrosion are less common external corrosion factors (Wasim et al., 2018).

Directly buried pipelines are most susceptible to corrosion sources such as sulphide cracking, microbial corrosion, electrochemical corrosion, atmospheric corrosion and exposure to stray currents (C. Wang et al., 2019a).

The probability of electrochemical corrosion increases significantly when the absolute level of the protective potential of the copper sulphate electrode decreases (below -0.85 V). In this respect, the probability of ECC occurring and spreading is higher in the sections between cathodic protection stations, where the protective potential is usually lower (Lyubchik et al., 2011) It has also been found that sections of pipelines close to steel mills, coal-fired power plants and livestock complexes are particularly susceptible to electrochemical corrosion (Lyubchik et al., 2011).

In addition, the potential for stress corrosion cracking (SCC) and ECC to occur is highly dependent on the corrosive activity of the soil. In acidic soils (pH < 5), the passivated magnetite film on the surface of pipes with broken insulation is either non-existent or weak, which increases the likelihood of stress corrosion cracking. At pH > 6, the passivated magnetite film is dense (especially in calcareous soils) and protects the pipe from ECC.

Stray currents are currents that are generated when the ground is used as a conducting medium and these currents deviate from their intended path. Depending on the source, they can be direct or alternating currents. Due to their low resistance, buried pipes tend to trap these currents, passing them along another route through themselves and subsequently withdrawing them underground, back to their original source. The conductive part of the buried pipe will be protected electrochemically, while the current-sharing part of the pipe may be susceptible to corrosion (Allahkaram et al., 2015; Qin et al., 2020; Solgaard et al., 2013).

Stray current corrosion poses a significant risk to the technical conditions for maintaining pipelines fit and safe for operation during the transportation of natural gas (Y. Wang et al., 2019), as the increased electrochemical reactions lead to a serious risk of accidents (Dann and Huyse, 2018; C. Wang et al., 2021a; Wang and др., 2020). Stray current-induced corrosion is characterised by high concentrations (Paul, 2016), and its characteristics are very different from natural corrosion. Stray current-induced electrochemical corrosion occurs at the interface between the soil electrolyte and the pipe surface, which contributes to the rapid degradation of the coating and the thinning of the pipe wall. The potential deviation causes electrons to bounce off the metal and complete the electrochemical reaction (C. Wang et al., 2019b).

At the same time the pipe wall is gradually depleted due to the cumulative effect of corrosion caused by stray currents, which is often accompanied by the onset of pitting. This can lead to perforation, which can cause leakage of the hydrocarbon product being transported (Wang et al., 2020).

The authors (C. Wang et al., 2021b)assessed the change in corrosion damage rate of natural gas pipelines due to the development of pitting corrosion caused by stray currents. The aim of the study was to establish a more reliable indicator for a timely response to the corrosion status of natural gas pipelines. A Monte Carlo model was

applied to describe the uncertainty in the effect of stray currents on corrosion losses. In this study, an integrated electrochemical method was developed for point estimation of the part of the pipeline most likely to experience stray current corrosion. This paper presents an integrated electrochemical approach to simulate the distribution of corrosion along a natural gas pipeline due to stray current leakage. This approach allows the temporal and spatial characteristics of the stray current corrosion distribution on the pipeline to be taken into account, which is important for predicting the locations on the pipeline where severe DC corrosion is particularly likely to occur. This helps to organise preventive measures to respond to corrosion conditions on natural gas pipelines in a timely manner and to improve the reliability of the pipeline.

As corrosion is a destructive process that varies over time and leads to the gradual depletion of metals, stray current corrosion is no exception (Dann and Maes, 2018) The degree of corrosion damage to pipelines by stray currents follows Faraday's law. This type of corrosion process is also influenced by many factors: stray current density, ion concentration in the electrolyte medium (Bertolini et al., 2007), pH (Qian and Cheng, 2017), applied strain, temperature (Yuan et al., 2018), etc.

The corrosion risk assessment of underground metallic pipelines is usually based on their potential, which is measured against a reference electrode. In the absence of stray currents, this measured potential has a constant value. When stray currents flow through the pipe, the system potential begins to fluctuate. Measuring changes in pipeline potential relative to the electrolyte and deviations from normal potential are the two main methods of detecting changes caused by stray currents and assessing their magnitude (Allahkaram et al., 2015).

Protective coatings are the first line of protection against corrosion to maintain the integrity of underground pipelines. They act as a physical and electrochemical barrier layer between the metal and the environment. If used properly, they can protect more than 99% of the pipeline surface (Farh et al., 2023).

An important aspect of corrosion protection and corrosion control methods for metallic pipelines buried in corrosive soils is the selection of a protective material for the particular corrosive environment. The material selected must meet certain criteria and requirements, namely: physical and mechanical properties, corrosion

and erosion resistance, design availability, cost, maintainability, compatibility with other system components, reliability and service life (Makarenko, 2009).

The thickness and resistivity of the protective layer are the main controlling parameters for its protective properties. However, its corrosion resistance and resistance to degradation vary depending on the permeability and chemical composition of the crude oil product, which may not be fully reflected by the above parameters (Xu et al., 2020).

Commonly used epoxy resins and carbon-based enamels exhibit cathodic protection from current flow, while high-performance composite coatings and polyethylene tapes block current flow in long-term tests (Kuang and Cheng, 2015). The authors have measured and modelled the environmental chemical and electrochemical characteristics of the electrolyte trapped under the protective coating (Yan et al., 2015). In addition, laboratory tests have been carried out to understand the protective behaviour of some gas pipeline coatings using electrochemical measurements, including constant potential currents and electrochemical impedance spectroscopy (Ruschau and Chen, 2006).

Defects in the coatings may be due to mechanical failures in the application of these coatings, negligence during operation, soil during backfilling of the pipeline, cracking due to increased mechanical loading, biological erosion in the soil, damage caused by subsequent construction works, etc. (Nykyforchyn et al., 2019, 2017; Wan et al., 2017). If the protective coating is damaged, stray currents begin to flow, resulting in a cathodic zone at the entrance and an anodic zone at the exit of the stray current path through the pipeline.

Due to delamination, degradation and defects from various causes, coatings lose their reliability over time, leading to corrosion. Therefore, coated pipelines must be combined with cathodic protection to prevent external corrosion (Shaalan et al., 2022). In addition, the coating makes the application of cathodic protection cost-effective and extends the life of the anode, as the coated pipeline requires less protective current. In other words, coatings and cathodic protection have a synergistic effect and complement each other (Brenna et al., 2020; Farh et al., 2023). While the coating provides a first barrier of protection against corrosion attack, cathodic protection acts as a back-up protection against coating defects (e.g.

perforations and dents) or corrosion damage in the event of coating failure (Chen et al., 2009; Kuang and Cheng, 2015)

However, depending on the nature of the defect and the chemistry of the pipeline environment, the cathodic current provided by cathodic protection can produce reaction products that affect the adhesion of the coating around the defect, leading to so-called cathodic stripping, which is considered to be the most important degradation mechanism for organic coatings on steel surfaces (Mahdavi et al., 2015; Xu et al., 2020).

In particular, when protective coatings are damaged, the following cathodic reactions occur: oxygen reduction and hydrogen release (Gu et al., 2020). Both reactions can be important causes of cathodic delamination of protective insulation coatings, but some studies have shown that it is hydrogen release that leads to greater delamination of the coating, so this process deserves more research in the pipeline field (Gu et al., 2020; Wang et al., 2022).

Cathodic protection (CP) refers to a method of protection in which a negative current is applied to a steel structure to shift the electrode potential towards the redox equilibrium potential of the metal by cathodic polarisation (Broomfield, 2020). The desired cathodic protection potential on the pipeline can be controlled manually (internal feedback) or semi-automatically (external feedback) (C. Wang et al., 2021a).

Cathodic protection systems polarise the steel surface of the pipeline and form a passive film (Kumar Thakur et al., 2021). Accepted conditions for preventing pipeline corrosion include a pipeline polarisation in the negative direction of greater than 850 mV (Brenna et al., 2014; Büchler, 2020; Kuang and Cheng, 2016).

Cathodic protection, as an active corrosion protection method, functions by applying a protective current that converts all the anodic (i.e., active) parts of a steel pipeline into cathodic (i.e., passive) parts (Farh et al., 2023). As the resistance between the pipeline and the ground increases, the current required for cathodic protection decreases.

To ensure effective cathodic protection of the pipeline, the following factors must be taken into account: pipe-to-ground potential, AC to DC current density ratio, AC voltage, AC current density. Experiments have demonstrated that the probability of

corrosion increases when the AC current density is between 30 and 100 A/m^2 and that considerable corrosion damage to the pipeline is more likely to occur when the density exceeds 100 A/m^2 (Goidanich et al., 2010).

In the case of AC, over-protection should be avoided, as it leads to an accelerated development of corrosion. The authors (Chen et al., 2020) have shown that the effect of AC corrosion is similar to that of steady-state AC corrosion as the intervention time increases. An increase in the ratio of AC current density to DC current density implies an increased risk of corrosion damage. In turn, a decrease in this ratio means that the probability of corrosion occurring is reduced, but it still does not guarantee complete prevention of corrosion.

When exposed to a corrosive medium at cathodic protection potential, cathodic failure usually starts with a coating defect, leading to the following electrochemical reactions (Mahdavi et al., 2017):

$$O_2 + 2H_2O + 4e^- 4OH^- \quad (3.1.1)$$

in case when the potential is less negative than -1100 mV;

$$2H_2O + 2e^- H_2 + 2OH^- \quad (3.1.2)$$

in case when the potential is more negative than -1100 mV.

These reactions produce hydroxyl ions which result in a highly alkaline environment near the coating defects. This high pH solution can lead to the onset of cathodic disintegration at the boundary of the coating defect (Mahdavi et al., 2017).

It is now recognised that the effectiveness of cathodic protection is achieved by activating the polarisation effect and the resulting concentration polarisation associated with oxygen reduction, as well as by increasing the pH of the steel surface (Brenna et al., 2020).

Cathodic protection can be carried out in two ways: by using a pulsed current and by using a metal protector anode. The first method does not require a power supply to provide current from the sacrificial anode to the protected part of the cathode. The condition is that the electrochemical potential of the anode metal must be higher than that of the cathode metal, which is the object to be protected – the pipe. The second method consists of generating the necessary current, for which a DC current

source – a rectifier (if AC power is available) or a diesel generator is used (Shaalan et al., 2022).

Cathodic protection with anodic grounding electrodes is defined as protection with electrically corrosive elements, in which the metal pipe acts as the cathode and the part to be corroded (sacrificed) is the anode in this system. Therefore, the anode is consumed and eventually needs to be replaced. The cathodic protection current of the metal pipe must be equal to the corrosion current of the anode grounding electrode (Szeliga, 2012).

However, cathodic protection systems with sacrificial anodes are not effective for protecting pipelines with low earth resistance (Szeliga, 2012). Furthermore, when pipelines are laid in cased pipes under road and railway tracks, the ability of the cathodic protection current to reach the protected pipe is mainly determined by the electrical insulation of the pipe and the cased pipe and the medium between them (Farh et al., 2023).

Pulsed current cathodic protection is a corrosion protection method that uses a sacrificial anode driven by an external direct current source (Broomfield, 2020). The positive terminal of the DC source is connected to the corrosion depleted anode and the negative terminal is connected to the steel pipe (cathode) (Mohammed and Abdulbaqi, 2018; Szeliga, 2012).

The extent of the external corrosion regime can be assessed by quantifying the rate of evolution of localised pipe damage. However, the full range of factors contributing to corrosion growth is poorly understood for environments with ventilated soils. Furthermore, over many years of operation, pipes are dynamically exposed to corrosive environments and the factors influencing the corrosion process tend to change over time (Cole and Marney, 2012; H. Wang et al., 2019).

The various criteria that can be used to assess pipeline defects treat corrosion as a localised thinning of the pipeline wall thickness and assess the resulting effect on mechanical stress and strain distribution (Qin and Cheng, 2021).

The integration of mechanical-electrochemical interactions in corrosion defects allows for physical modelling that can contribute to more accurate defect assessment and possible pipeline failure prediction at a more mechanical level. For example, the authors (Xu and Cheng, 2013) presented the concept of mechanical

and electrochemical effects of pipeline corrosion: they derived theoretical dependencies between the thermodynamic component of corrosion (i.e., electrochemical equilibrium potential), the kinetic component (i.e., anodic and cathodic current densities), and the mechanical stress and strain of the corroding steel, and confirmed these dependencies with experimental data (Liu et al., 2011; Xu and Cheng, 2012; Yang and Cheng, 2016).

In connection with the expediency of increasing the useful life of pipeline transport, it is necessary to take into account the fact of the negative effect of the stress state of the pipe metal, which contributes to the development of electrochemical corrosion. The presence of residual stresses in the pipeline wall, both tensile and compressive, leads to the appearance of local areas of plastic deformation. This, in turn, significantly enhances the spread of the corrosion process in the metal, which can cause premature failure of the object. Therefore, it is necessary to establish a clear relationship between the corrosion rate and the degree and type of plastic deformation of the pipe metal. This dependence is also necessary to determine the deadline for the use of the pipeline.

The authors (Bolobov et al., 2022) also investigated the effect of mechanochemical effects by calculating corrosion rates under different types of loading. Using pipeline steel 17GS (Fe510D1) as an example, it was found experimentally that electrochemical corrosion of metals is most intense when objects are subjected to tensile stresses and also when stress concentrators are present.

As major gas pipelines are single objects consisting of individual parts welded together to assemble a transport system, it is important to note that the presence of corrosion defects at the weld seams poses a significant threat to the integrity of the pipeline. These defects may be the result of welding, or they may be the result of corrosion during the operation of the pipeline, as the weld joint is a stress concentrator (Qin and Cheng, 2021). Due to the complex composition, structure, resulting stresses and electrochemical properties, corrosion defects in pipeline welds must be modelled using a large amount of input data and involving a large number of physical fields. As a result, predicting the fracture process in pipeline welds may be more difficult to simulate. To date, there has been little research on this topic (Teran et al., 2019; Yeom et al., 2016).

However, the most common internal corrosion factors in oil and gas systems are corrosive gases (e.g., CO_2 and H_2S) (Folena and Ponciano, 2020), elevated pressure, temperature, flow rate, and pH (Ben Seghier et al., 2022; Benitez et al., 2002).

The presence of H_2S hydrogen sulphide in oil and gas fields can affect the metallurgical properties of structural steel, such as ductility, leading to a loss of mechanical properties. Hydrogen embrittlement is a related process that can lead to catastrophic pipeline failures. The operating conditions of pipelines, i.e., high temperatures, pressures and flow rates, combined with the presence of hydrogen, lead to the necessary conditions for hydrogen embrittlement and hydrogen-induced cracking (Folena and Ponciano, 2020).

When using steel for the manufacture of hydrocarbon transport pipeline systems, account must be taken of the fact that pipeline steel is susceptible to material degradation in the presence of hydrogen. And one manifestation of this fact is the growth of fatigue cracks in the presence of hydrogen. Understanding the extent to which hydrogen accelerates the growth of fatigue cracks has been the subject of much research (Alvaro et al., 2019; Ronevich et al., 2018; V. Singh et al., 2019).

Hydrogen embrittlement is a phenomenon of accelerated fracture caused by the introduction of hydrogen during fabrication or repair (Nagumo, 2016; Robertson et al., 2014). This phenomenon can be caused by the embrittlement of aggregated hydrogen molecules or hydrides, or it can occur suddenly at low loads, with very low hydrogen concentrations, after a long delay (Z. Wang et al., 2021). The latter leads to catastrophic failure of steel and other structural materials under natural gas and hydrogen transport conditions (Bai et al., 2020; Chatzidouros et al., 2019; Koyama et al., 2017).

Despite significant improvements in the understanding of the hydrogen embrittlement and a wealth of experimental data on the behaviour of metals during hydrogen, a number of key issues in this process remain relevant. For example, predicting the sensitivity of metals to HE under specific industrial conditions remains challenging because of the problems in accurately determining the interaction between absorbed hydrogen and metal microstructure under different environmental conditions (Li et al., 2022). Predicting hydrogen sensitivity requires knowledge of the properties of the material itself (e.g., crystal structure, grain

boundaries, dislocations, inclusions) and the external conditions that determine hydrogen exposure (e.g., temperature, humidity, pH and pressure) (Zhang et al., 2023).

In their study Zhou et al. (Zhou et al., 2021) conducted tensile experiments on both smooth X80 pipe steel specimens and notched specimens. The yield strengths of the base metal of X80 pipeline steel measured in the experiments in a reference atmosphere and three simulated atmospheres with hydrogen volume fraction of 1%, 2.2% and 5% were 660.9 MPa, 668.1 MPa, 676.5 MPa and 659.1 MPa, respectively. The yield strength of the sample reaches its maximum in an atmosphere with hydrogen content of 2.2%. However, the yield strengths at all 4 atmospheres were practically identical. When the material entered the plastic stage, the stress began to increase slowly with increasing strain. The tensile strengths were 724.2 MPa, 726.7 MPa, 727.5 MPa and 722.2 MPa, and the corresponding strains were within 5-6%, as shown in Figure 2. Thereafter, the stress gradually decreased and the specimens finally failed when the strain reached the range of 16%-18%. It can be concluded that the addition of hydrogen has no significant effect on the tensile strength of X80 pipe steel, but has a significant effect on the yield strength.

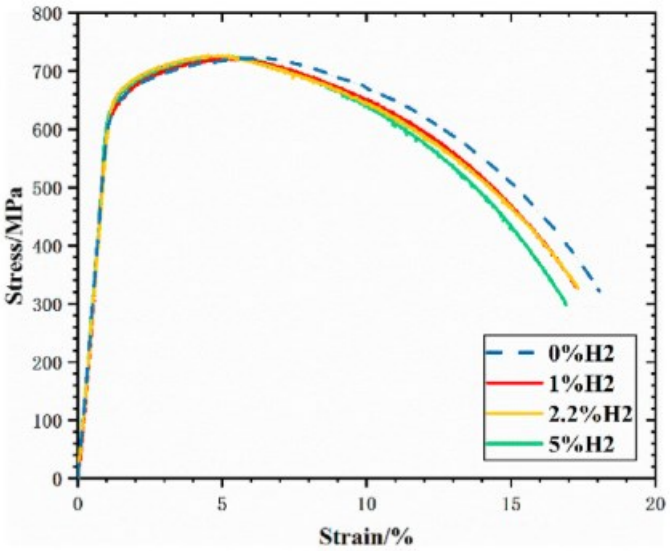

Figure 2: Tensile diagram under slow loading of smooth round bar specimen (Zhou et al., 2021)

High-strength steel pipelines are widely used to transport hydrocarbons over long distances (Laureys et al., 2022; Nanninga et al., 2010). It is known that hydrogen embrittlement problems occur when the interior of the pipeline is exposed to high

pressure hydrogen (Ghosh et al., 2018; Ohaeri et al., 2018) or acidic gases containing hydrogen sulphide H_2S, due to the acidic corrosion of the steel and the production of hydrogen atoms (Mohtadi-Bonab et al., 2021). However, hydrogen embrittlement can also occur when the outer surface of the pipe is exposed to electrochemically generated hydrogen due to cathodic protection (Cazenave et al., 2021; Zhang et al., 2018). In some cases, the inner and outer surfaces of a steel pipeline can be exposed to hydrogen from different sources at the same time.

Since hydrogen embrittlement can be caused by both internally dissolved and environmentally adsorbed hydrogen atoms, Lynch (Lynch, 2012; Z. Wang et al., 2021) proposed the adsorption-induced dislocation emission (AIDE) mechanism. In AIDE, hydrogen atoms diffuse to the internal apex of a stress-induced crack or adsorb from the environment to the outer surface of the crack. These atoms enhance the emission of dislocations within a few nanometres of the crack tip and are rapidly carried away by these dislocations.

Nagumo (Nagumo, 2016; Nagumo and Takai, 2019; Z. Wang et al., 2021), on the other hand, described the interaction of strain amplitude, the presence of hydrogen and vacancies, and proposed a mechanism for hydrogen enhanced strain-induced vacancies (HESIV). According to this theory, the combination of hydrogen atoms and vacancies in the plastic zone of the metal reduces their mobility and stabilises these vacancies, thereby localising deformation and forming clusters.

Wang et al. (Z. Wang et al., 2021) argue that the local distribution of hydrogen affects the brittleness of α-Fe single crystals and that dissolved and adsorbed hydrogen atoms in particular cause hydrogen embrittlement in steel, which in turn is partly based on the mechanisms of hydrogen enhanced local plasticity (HELP) (Schippl et al., 2018; R. Singh et al., 2019) and hydrogen enhanced strain enhanced vacancies (HESIV) (Z. Wang et al., 2021).

In addition, the hydrogen enhanced debonding (HEDE) mechanism has been suggested as a representative mechanism for HE (Traidia et al., 2018). The HELP model is based on the idea that hydrogen promotes dislocation movement and thus reduces local shear strength, i.e., hydrogen diffuses into the crack tip region and hydrogen atoms are attracted to the lattice strain around the dislocation, which in turn migrates to the lower stress region, thereby increasing its mobility. On the other hand, the HEDE model assumes that the atomic bonds in front of the crack tip are

weakened by stretching the atomic lattice due to the presence of hydrogen, and therefore the fracture energy is reduced (Li et al., 2018). HEDE is thought to dominate when brittle fracture surfaces are observed, whereas HELP is seen more as a highly localised plastic fracture process.

Also, H_2S sulphide is known to be responsible for cathodic reactions on the steel surface of the pipeline, due to the release of hydrogen atoms and sulphide ions into the environment (Folena and Ponciano, 2020). The hydrogen atoms diffuse easily into the crystalline matrix of the steel due to their small size. These atoms are then trapped and accumulate in the form of lattice defects such as micro voids, vacancies, dislocations, inclusions and segregation zones, leading to the formation of cracks (Mohtadi-Bonab et al., 2013). This hydrogen-induced cracking can even start without significant external stresses, but intensifies as the ductility of the metal decreases in response to tensile stresses. On the surface of the pipe, sulphide ions can combine with iron ions released by the dissolution reaction of the iron anode to form iron sulphide. The iron sulphide formed on the steel surface can in turn act as a diffusion barrier, weakening the corrosion rate and/or absorbing hydrogen.

The kinetics of damage generated by vacancy clusters are closely related to the strong localisation of strain, for example, near grain boundaries. Characteristics of hydrogen embrittlement mechanisms in steel, such as sensitivity to microstructure, fracture morphology and strain rate and temperature dependence, correlate well with damage kinetics (Nagumo and Takai, 2019). Zhang et al. (Zhang et al., 2018), stated that the sensitivity of pipeline steels to hydrogen embrittlement should also be determined by the variation of the fracture surface and not only by an empirical value based on the degree of hydrogen embrittlement.

The presence of H_2S, i.e., acidic hydrocarbons, is one of the most prominent causes of failure and defect formation in carbon steel pipelines. most of the atomic hydrogen produced by the electrochemical corrosion reaction between H_2S and iron penetrates into the base material through an adsorption-absorption-diffusion mechanism (Hao et al., 2018; Tian et al., 2018). At defective interfaces in steel in the form of elongated non-metallic inclusions (e.g., MnS sulphide), diffused hydrogen is trapped and forms gaseous hydrogen cavities under high pressure. The increase in pressure within these cavities is continuously supported by the hydrogen from the corroded steel surface, which is the main driver for the formation and

growth of small cracks, i.e., hydrogen-induced cracking (HIC) occurs (Gan et al., 2018).

Furthermore, in addition to the corrosive effects of hydrogen sulphide, corrosion in a carbon dioxide environment is one of the important and dangerous types of damage to objects in straight sections of trunk pipelines, accelerating their corrosive damage (Shaposhnikov et al., 2022). According to the analysis of statistical data on the accident rate of trunk pipelines transporting natural gas, one of the main causes of failures is damage caused by corrosion of carbon dioxide (Shaposhnikov et al., 2022).

Compared to hydrogen sulphide (H_2S), CO_2 was earlier considered a minor player in ecological corrosion in natural gas production (Devyaterikova et al., 2019). With the development of deep natural gas condensate fields with reservoir temperatures above 80°C, pressures above 30 MPa and CO_2 content in the gas above 1 vol%, the issue of CO_2 corrosion has become increasingly important (Artemenkov et al., 2017).

It is worth mentioning that currently scientists are very interested in the implementation of new technologies and the development of methods to solve the problem of corrosion damage in hydrocarbon feedstock pipelines, optimise CPS operations and develop means of electrochemical protection, in particular - anode grounding devices.

An analysis of patents on international scientific developments shows the following results. Thus, for example, the useful model represented in patent (Redekop, 2022) relates to the field of electrochemical protection and creates protection of underground pipelines for liquid and gas transport with application to pipeline transport. The technical results of this model, including the increased reliability of the operation of anodes in electrochemical protection systems, are achieved by the presence of a conductive shell and a conductive core in the anode, made of copper wires and flexible graphite-containing ropes in contact with each other.

Similar to the above model is the utility model (Odegov et al., 2019). The device contains a metal conductor, a polymer sheath, an additional titanium electrode, a mineral sheath, a conductive sheath and a woven bag. The titanium electrode is coaxial with the metal conductor in the mineral sheath; and depending on the length

of the anode ground electrode, there can be several titanium electrodes. The metal conductor is made of flexible copper wire. The mineral sheath is made of carbon filler with graphite powder. The technical problem solved by the utility model is to increase the mechanical tensile strength of the device. Nevertheless, the disadvantage of this device is its low reliability. This is due to the fact that the utility model uses copper wire as the core, which has a high solubility in the presence of electric current, and if the copper wire is damaged, the electrochemical protection zone is reduced. When the sheath is damaged, the destruction of the copper wire is accelerated. Placing the titanium electrode close to the metal conductor will reduce the level of electrochemical protection because the titanium electrode and the metal conductor will act as two separate anodes, generating their own electric fields and interfering with each other. In addition, the titanium electrodes are hard and inflexible, which can cause the integrity of the sheath to be compromised when the grounding electrode of the anode is bent.

A flexible anode model is also described in a patent by scientists from China (Yanqiang et al., 2017). The model device consists of a copper core cable, anode wire, coke filler, air tube, fabric mesh and fibre optic sheath. This model has a connection point to the anode wire, the copper wire cable. This cable, the anode wire and the gas pipe are coaxially located in the coke loader. The gas pipe diverts the gas generated in the casing and the grid. However, due to the use of copper cores, this model also has a disadvantage because, as mentioned above, copper has a high solubility in the presence of current. As a result, when the copper core dissolves, the electrochemical protection area is reduced. In addition, if the copper cores are not connected tightly enough, the working range of the device is reduced, which also leads to reduced reliability.

Another invention by Russian scientists (Aginey et al., 2020) was aimed at saving resources when installing and operating an anode earthing, which is part of a cathodic protection device for gas pipelines laid underground. After drilling a borehole parallel to the structure to be protected and below the water table, the pipe is installed into it, consisting of two connected half-cells, made of materials with different resistances. When installing the pipe, the pipe is rotated so that the half-cells of the highly resistive material face the protective earth. A structure consisting of two half-cells welded together is connected to the tube of conductive material,

into which the protective electrodes are pulled via a cable and filled with a conductive solution. The technical result of the invention is an increase in the service life of the anode earthing under conditions where the protective earthing and lightning protection system components have a negative impact on the current distribution parameters of the cathodic protection system.

The object of the present invention (Kajiyama, 2008) is a system for preventing corrosion in pipelines with a high resistance coating based on electro-anodes. The system comprises a probe for determining the target protection area of the pipeline. The current generated by the electroplated anode is set so that the potential of the probe to be disconnected is less than the corrosion prevention potential. The present invention (Goodwin, 2019) also relates to the field of corrosion protection of pipelines. The model relates to a method of manufacturing an electroplated anode containing a spiral coil and expendable metal.

The aim of the invention (Aginey et al., 2019) is to estimate the remaining service life of electrochemical corrosion protection elements for underground pipelines. This useful model can be used to determine the service life of anodes for earthing and to determine the period of their repair or complete replacement.

The authors (Liang et al., 2023) and (Liu et al., 2023) investigated the effectiveness of using anode earthing made of zinc or indium alloys and anodes made of magnesium alloys, respectively, in the cathodic protection of pipelines against corrosion. The studies proved that the use of these anode grounding electrodes is an effective solution against AC corrosion.

Furthermore, the aim of the invention (Politov, 2019) is to improve the design of anode earthing for the electrochemical protection of metallic structures against corrosion when in contact with highly resistive soils. The proposed anode earthing electrode, the body of which is made of a conductive polymeric material, is made in the form of a tube with a plurality of perforations. This technical solution contributes to a significant increase in the reliability and service life of the electrode, as the low solubility of the polymeric material eliminates the possibility of forming an oxide film and resists aggressive environments, in contrast to similar devices where the metal core is dissolved during the protection process. The dissolution of the metal core leads to a deterioration of the electrical parameters of the anode earthing electrode and a significant increase in current resistance. In addition, the presence of

perforations in the electrode body contributes to the uniform wetting of the electrode body surface by the activator solution, thus providing a reduction in transient resistance, which increases the efficiency of the anode earthing electrode.

3.2 Methodology

In most cases, cathodic protection stations operate in a protective potential maintenance mode, which is not adapted to changing load conditions. As the protection potential is only monitored at the point of discharge and does not take into account changes in the corrosive environment and the equipment protecting the pipeline, increasing the maximum protection potential of a section of pipeline can lead to undesirable consequences such as deterioration of the mechanical properties of the pipeline metal, an increase in the dissolution rate of the anode grounding and delamination of the protective insulation coating.

An analysis of the latest scientific studies, specifications and technical documents in the field of condition monitoring of pipelines and their electrochemical corrosion cathodic protection shows that the selection of the optimum mode of operation of the elements of the electrochemical protection system, taking into account the influencing factors and their combination, is an urgent and important task.

The existing CPS operation regulation methods are oriented towards specific local sites and industrial objects. In industrial sites, the cathodic protection current field is inhomogeneous, so existing methods treat the protected object as a system of points where the protection potential is measured[4]. For each particular point, a dependence coefficient between the protection potential difference and the CPS influence current value is determined. In turn, the influence coefficient is found by regression analysis.

According to the results of the study (Fatrakhmanov, 1998), the variation of the protection potential difference is related to the magnitude of the CPS current at each particular point with sufficient and high predictive power, described by a system of linear equations:

[4] *STO Gazprom (Proprietary Standard) 9.2-002-2009 Protection against corrosion. Electrochemical protection against corrosion. Basic requirements - Introdused 2009-10-13*, 2010

$$\left.\begin{array}{l}\varphi_1 = A_{01} + A_{11}I_1 + A_{21}I_2 + \cdots + A_{i1}I_n \\ \varphi_2 = A_{02} + A_{12}I_1 + A_{22}I_2 + \cdots + A_{i2}I_n \\ \varphi_k = A_{0k} + A_{1j}I_1 + A_{2j}I_2 + \cdots + A_{ij}I_n\end{array}\right\}, \quad (2.2.1)$$

φ_i – potential difference of the i^{th} point of the industrial site, where i=1; 2; … k;

I_j– the current of the j^{th} cathodic protection station, where j =1; 2; ...k;

A_{ij}– the coefficient of influence of the n^{th} CPS on the total potential difference at the measuring point.

The above set of equations for k points and n CPS at an industrial site is used to solve the current regulation problem for cathodic protection devices in order to find the optimal mode. This problem is the minimisation of the output power of all active CPS used to protect the pipeline:

$$\sum P_j = \sum_{j=1}^{m} I_j^2 \cdot R_j, \quad (2.2.2)$$

I_j – the current intensity of the j^{th} CPS;

R_j – impedance of the external circuit of the j^{th} CPS

It is important to observe the limitations on potential differences:

$$|\varphi_{min}| \leq |\varphi_i| \leq |\varphi_{max}|, \quad (2.2.3)$$

φ_{min}, φ_{max} – the minimum and maximum permissible protective potential differences at the points determined in accordance with the technical regulations.

A feature of this approach is that the optimum operation of the cathodic protection station does not take into account the corrosion factors of the object to be protected and their combination. Furthermore, in order to determine a model for the dependence of the distribution of the protection potential difference on the intensity of the current generated by the CPS, i.e., to find the influence coefficient A_{ij}, it is necessary to determine a fixed potential A_{0j}. This parameter is determined by the inherent potential of the gas pipeline metal when all switches affecting the CPS, and when the pipeline is depolarised. The value of the potential of the pipeline itself is influenced by the chemical composition of the pipeline metal and the chemical properties of the surface where the pipeline is located.

Depolarisation of an operating pipeline with a good insulating coating condition is difficult to achieve. This process can take several days at the measurement point and can be interfered with by the operation of other operating CPS. This method is therefore impractical as it requires a large number of cathodic protection stations to be shut down for long periods of time, resulting in increased logistical costs. Another disadvantage of this model is that it requires a large amount of background information, such as operational cathodic protection potential data obtained through regular measurements.

The method described does not take into account the influence of important factors such as the condition of the insulation coating on the potential distribution, the inevitable changes in the chemical composition of the environment during operation and the cumulative effect of corrosive factors.

In order to eliminate all the above-mentioned drawbacks, new methods for distributing the protective potential along the pipeline need to be developed. Therefore, S.A. Nikulin (Nikulin et al., 2014; Nikulin, 2015) proposed a method for determining pipeline shielding which excludes the above-mentioned drawbacks. In this method, it is proposed to use the introduced external potential difference parameter instead of the CPS system's own potential A_{0j}. The method consists of determining the coefficient of CPS influence on a point and calculating the external potential difference at the “pipe-ground” point as the difference between the total potential difference at that point and the total revealed value of CPS influence.

In order to calculate the external potential difference at the “pipe-ground” point, the protective total potential difference at the drainage point (360 km CPS) must be measured in the following order:

1. the CPS is switched off;
2. the total protection potential difference at the selected drain point is measured with reference to a fixed copper sulphate reference electrode;
3. next, the current intensity at the CPS outlet shall be measured;
4. after this, the CPS shall be opened;
5. the CPS output current shall then be increased according to the selected control step (1 A);
6. repeat steps 2-5 until the current value is 13 A;

7. repeat steps 1-6 *n* times.

As the external potential difference includes a component determined by the output parameters of the joint station, for the investigation point it is necessary to find the coefficient of influence of the joint station on the total protection potential difference. The measurements for all adjacent CPS (at km 336, 345, 371, 384) are to be carried out in the following order:

1. the adjacent CPS is switched off;
2. measuring the total protection potential difference at the measured drainage point with respect to a fixed copper sulphate reference electrode;
3. the current output from the adjacent CPS is measured;
4. the adjacent CPS is switched on;
5. the current output from the CPS is increased by the control step – 3 A;
6. repeating steps 2-5 until the current value is 21 A;
7. repeating 1-6 *n* times.

Once all the impact factors for CPS have been determined, the following equation is derived:

$$\varphi_1 = \varphi_{st} + A_{11}I_1 + A_{12}I_2 + \cdots + A_{ij}I_n, \quad (2.2.4)$$

φ_{st} – steady-state pipeline potential, V;

φ_1 – total protective potential difference, V;

I_n – output current of the n^{th} RMS, A

From the resulting equation, the steady-state pipeline potential is expressed. As the effects of all CPS and current sources have not yet been determined, this potential is expressed using the value of the external potential difference “pipe-ground”, which includes the steady-state potential and the potential applied by the unknown source:

$$\varphi_{external} = \varphi_{st} = \varphi_1 - A_{11}I_1 - A_{12}I_2 - \cdots - A_{ij}I_n, \quad (2.2.5)$$

$\varphi_{\text{стор}}$ – external potential difference of the gas pipeline, V.

Anode dissolution, high electrochemical activity and internal corrosion resistance for almost any application environment.

In underground main gas pipelines, where the ground resistivity is less than 100 Ohm·m, the use of extended grounding anode is recommended[5].

In general, the construction of an extended grounding anode should consist of an electrode, a working element, a connecting conductive cable and a contact node. The connection point of the electrode should be reliably isolated from the electrolytic contact with earth. The design should provide for connection on one or both sides of the cable terminals for connection to the terminal clamps of the instrumentation terminal block. The design of reinforced extended grounding anode, on the other hand, must include, for example, a metal braid on the sheath of the electrode working body, a reinforced core on the structure of the electrode conductor, etc. The design of the extended grounding anode electrode must ensure uniform wear of the working element material over the entire surface.

Due to the inadequate performance of steel deep grounding electrodes, they are used as anode grounding electrodes in the 336-384 km CPS of the “Punga-Ukhta-Gryazovets III” main gas pipeline. In order to improve the operational efficiency of the CPS, it is recommended to use an extended elastomeric grounding anode electrode of the ELER-2.1 series. This grounding element consists of a conductor wire and a working sheath made of a conductive elastic material with a constant specific resistance value in the range of 0.5 to 5 Ohm·m.

Elastomeric grounding anode electrodes are used for the uniform distribution of the protective potential over the surface of the pipe. They are a cylindrical linear electrode consisting of 1-2 conductive shells with a metal core inside as a current conductor (Kopytin, 2005). The core is coaxial with the central axis of the electrode.

The efficiency of these electrodes is due to the protective current distribution principle in the “pipe-anode” system, i.e., the current is only distributed in the ground volume between two parallel linear electrodes – the pipe and the anode grounding electrode – which allows for a current distribution factor of no more than 100% (Kopytin, 2005).

---

[5] *State Standard GOST R 58344-2019 Earthing switches and grounding devices for various purposes. General technical requirements for anode grounding of electrochemical corrosion protection installations - Introduced 2019-06-01*, 2019

In addition, the current density becomes progressively more uniform along the entire length of the anode during operation, which ensures uniform depletion of the ground electrode along its entire length (Delektorsky and Stefov, 2006).

The calculation of the basic electrical characteristics is based on the regulatory document[6] and is presented in section 3.2.

3.3 Theoretical and experimental research

For this study, we have chosen a 336-384 km section of the Punga-Ukhta-Gryazovets III gas pipeline. The pipeline crosses swampy land with alternating sandy soils and peatlands interspersed with organic matter.

In order to determine the number of experiments, it was necessary to use the planning theory of the experiments. This planning problem is described by the following model:

$$y = f\,(x_1, x_2, \ldots x_n), \qquad (2.3.1)$$

y – the dependent variable of the response,

x_i – the factors affecting the response, which may change during the experiment.

In this system, the value of the protection potential at the CPS drain point is taken as the response and the value of the current intensity at the output of each i^{th} CPS is taken as the factor.

For the linear regression model chosen, the number of experiments performed *n* coincides with the number of linear regression equation coefficients *k+1* (in this case *k* equals A_{ij}) and will therefore be determined by the number of CPS on the main gas pipeline segments considered.

In the technical section considered, five CPS, designed for a nominal output current of 21 A, were used. Therefore, the number of experiments required in this case would be 6.

[6] *RD 106-05. Rules for use of elastomeric anode grounding electrodes in cathodic protection installations and protective earthing circuits.*, 2005

Before proceeding to construct a model for the variation of the protection potential at the drainage point by means of linear regression analysis, we carry out a calculation of the cathodic protection device. This calculation is carried out according to a number of regulations. First, we calculate the electrical characteristics of the pipeline being protected. The initial data for a given section of the main gas pipeline divided into five sections by five CPS are presented in Table 1.

№ section / **Parameter**	**1**	**2**	**3**	**4**	**5**
Pipe diameter, mm	1420				
Wall thickness, mm	17				
Pipe steel grade	17GS (Fe510D1)				
Type of insulation coating	bitumen mastic + polymer tape				
Electrical resistivity of pipeline metal, Ohm·m	$2.45 \cdot 10^{-7}$				
Depth of pipeline, m	1.5				
The average electrical resistivity of the ground, Ohm·m	44.2	51.33	48.18	54.35	47.51
Length of protected parts, m	9000	15000	11000	13000	5000
Initial insulating coating resistance, Ohm·m^2	150000				

Table 1: Input data

1. Longitudinal pipeline resistance R_p, Ohm/m, is calculated according to the formula

$$R_p = \frac{\rho_p}{\pi(D - \delta_p)\delta_p}, \tag{3.3.2}$$

D – pipeline diameter, m;

δ_p – wall thickness, m;

ρ_p– electrical resistivity of pipeline metal, Ohm·m.

2. Current flow resistance of the pipeline, Ohm·m^2:

$$R_r = \frac{\rho_{gr} \cdot D}{2} \cdot \ln \frac{0{,}4 \cdot R_r}{D^2 \cdot H_p \cdot R_p}, \tag{3.3.3}$$

ρ_{gr} – the average electrical resistivity of the ground, Ohm·m;

H_p– depth of pipeline, m

Since the expression is transcendental, the solution to the problem of determining the current flow resistance of the pipeline is done using software products (in this case, MathCAD).

3. The transient resistance of the pipeline (at the time *t*) per unit length is calculated using the following formula

$$R_t = \frac{R_0 e^{-\beta t} + R_{\text{r}}}{\pi D}, \tag{3.3.4}$$

R_0 – initial insulation resistance of the gas pipeline, Ohm·m^2;

β – a coefficient specifying the rate of change of insulation resistance over time (to be selected depending on the type and design of the insulation, and depending on the operating conditions of the pipeline – normal or extreme), β = 0.11, 1/year;

t – the lifetime of the pipeline, *t* = 43 years.

4. Current propagation constant along the gas pipeline:

$$\alpha_p = \sqrt{\frac{R_p}{R_{\text{t}}}} \tag{3.3.5}$$

5. Inlet pipeline resistance:

$$Z_{\text{c}} = k_z \sqrt{R_p R_{\text{t}}} \cdot \text{cth}\left(\alpha_{\text{c}} \cdot k_z \cdot L_{\text{p}}\right), \tag{3.3.6}$$

k_z – construction constant of the CPS (k_z=1, for cantilevered asymmetrical anode connection scheme; k_z = 0.5 – for symmetrical anode connection scheme);

L_{p} – length of protected pipeline's parts, m

The results of the calculation of the electrical characteristics of the main gas pipeline to be protected are shown in Table 2.

№ section / **Parameter**	**1**	**2**	**3**	**4**	**5**
Longitudinal pipeline resistance, Ohm/m	$3.27 \cdot 10^{-6}$				
Current flow resistance, Ohm·m^2	118.69	139.19	130.14	147.89	128.21
The transient resistance of the pipeline, Ohm·m	323.554	328.151	326.122	330.102	325.689

Current propagation constant, 1/m	$10.05 \cdot 10^{-5}$	$9.98 \cdot 10^{-5}$	$10.01 \cdot 10^{-5}$	$9.95 \cdot 10^{-5}$	$10.02 \cdot 10^{-6}$
Inlet pipeline resistance, Ohm	0.045	0.036	0.041	0.038	0.070

Table 2: Calculated electrical characteristics

3.3.1 Modelling the change in protective potential at the drainage point using the linear regression analysis method

There are various ways to study statistical groups of random variables, such as variance, correlation and regression analysis. Variance analysis determines the effect of a particular factor on the process under study based on statistical data. Correlation analysis assesses the strength of the relationship between variables, while regression analysis helps to select a mathematical model and assess its adequacy for the established relationship between random variables (Kobzar, 2006).

Based on the data presented in the Annex tables 1-5 for the 336-384 km section of the main gas pipeline, linear regression analysis was used to construct a model for the dependence of the drainage points of the 360 km CPS on different values of current strength at the CPS outlet. This approach reveals the functional form of the relationship between the protective potential difference and the current intensity of the CPS.

The linear regression analysis is based on this relationship:

$$y = \alpha + \beta x, \qquad (3.3.1.1)$$

α and β – unknown regression coefficients.

Since the calculation of regression equation coefficients by the method of least squares can be applied to any statistical data distributed according to any law (Rebrova, 2016), we apply this method.

The method of least squares is based on the requirement to minimize the sum of squares of deviations of experimental points from the corresponding values of the regression equation:

$$S = \sum_{i=1}^{n} [y_i - \hat{y}_i]^2 = min \qquad (3.3.1.2)$$

Thus, equation (2.3.1.1) takes the form of the following system of equations:

$$\begin{cases} \sum_{i=1}^{n} y_i - \sum_{i=1}^{n} (\alpha + \beta x_i) = 0 \\ \sum_{i=1}^{n} y_i x_i - \sum_{i=1}^{n} (\alpha + \beta x_i) x_i = 0 \end{cases} \qquad (3.3.1.3)$$

Solving the system of equations gives the required regression coefficients:

$$b = \frac{n \sum_{i=1}^{n} y_i x_i - \sum_{i=1}^{n} x_i \sum_{i=1}^{n} y_i}{n \sum_{i=1}^{n} x_i^2 - (\sum_{i=1}^{n} x_i)^2}; \qquad a = \frac{\sum_{i=1}^{n} y_i - b \sum_{i=1}^{n} x_i}{n} \qquad (3.3.1.4)$$

In the following, the models of dependencies of the measured value of protective potential on the current strength are presented (Figures 3-7) using the data presented in the Annex tables 1-5. The linear regression analysis problem was solved using machine learning library – “Scikit-Learn” written in Python programming language and, directly, using “LinearRegression” class from “sklearn.linear_model” package used for linear regression implementation.

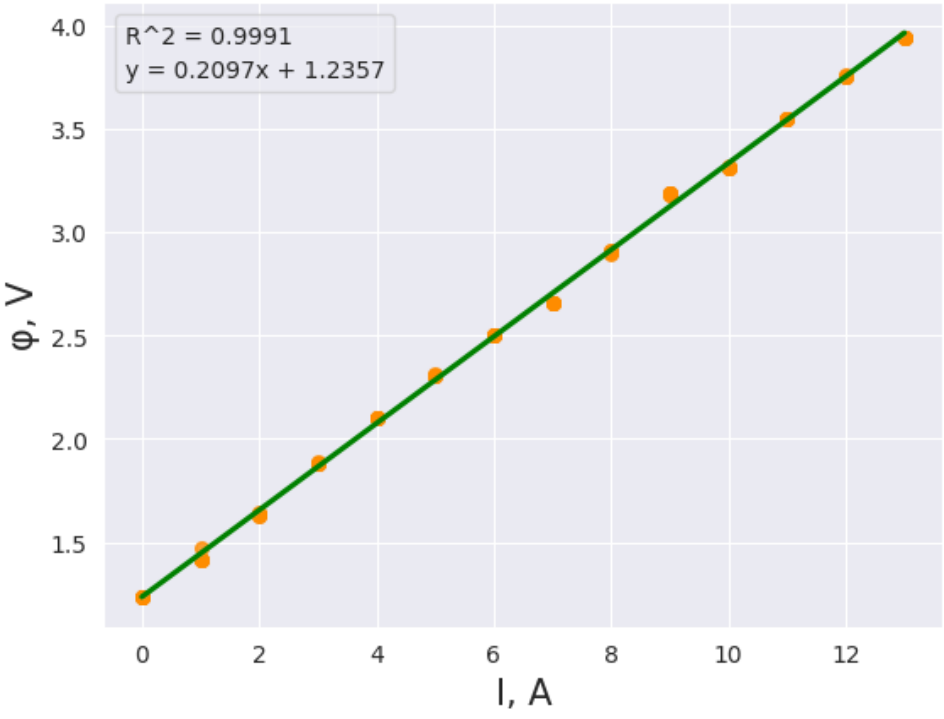

Figure 3: Plot of the impact of the 360 km CPS on the protective potential difference

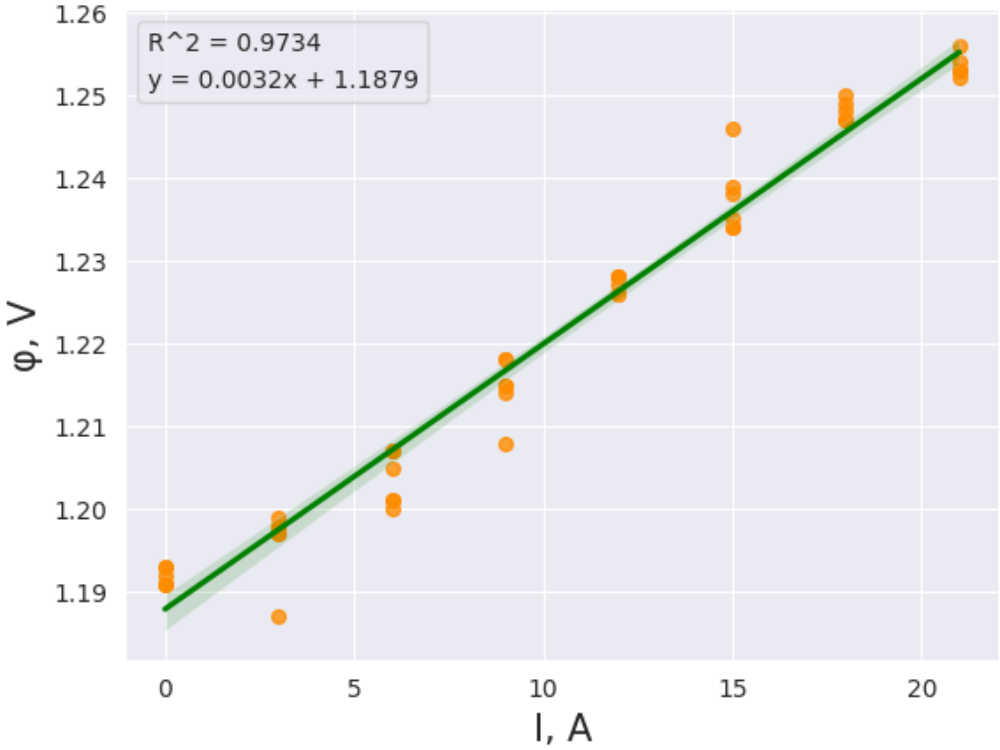

Figure 4: **Plot of the impact of the 336 km CPS on the protective potential difference at the 360 km CPS drainage baseline**

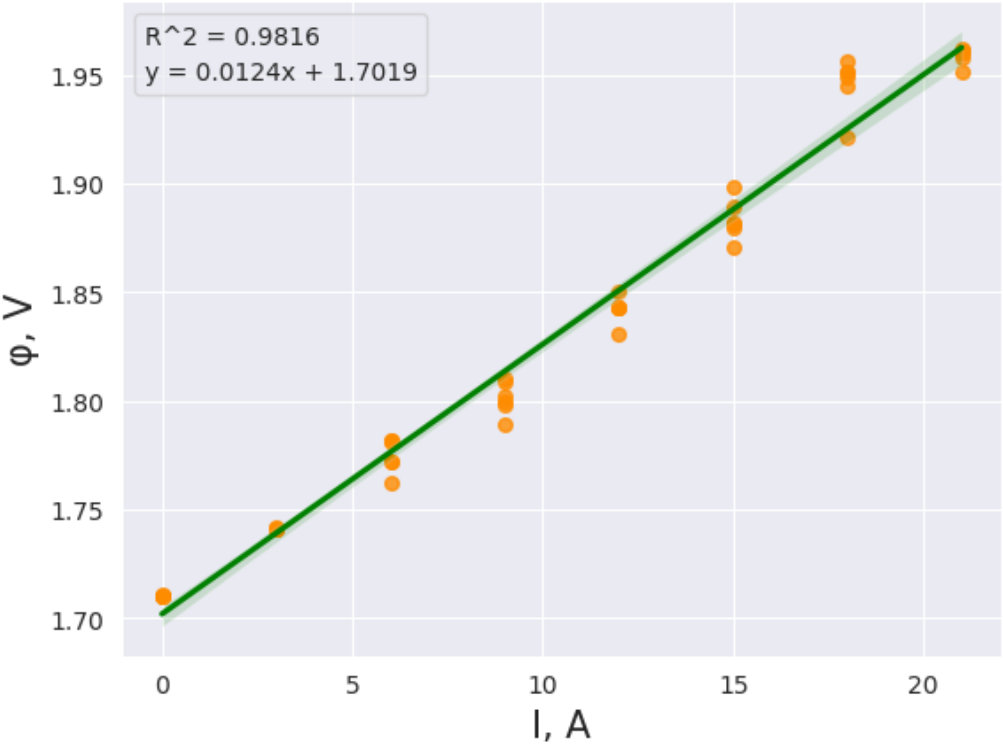

Figure 5: **Plot of the impact of the 345 km CPS on the protective potential difference at the 360 km CPS drainage baseline**

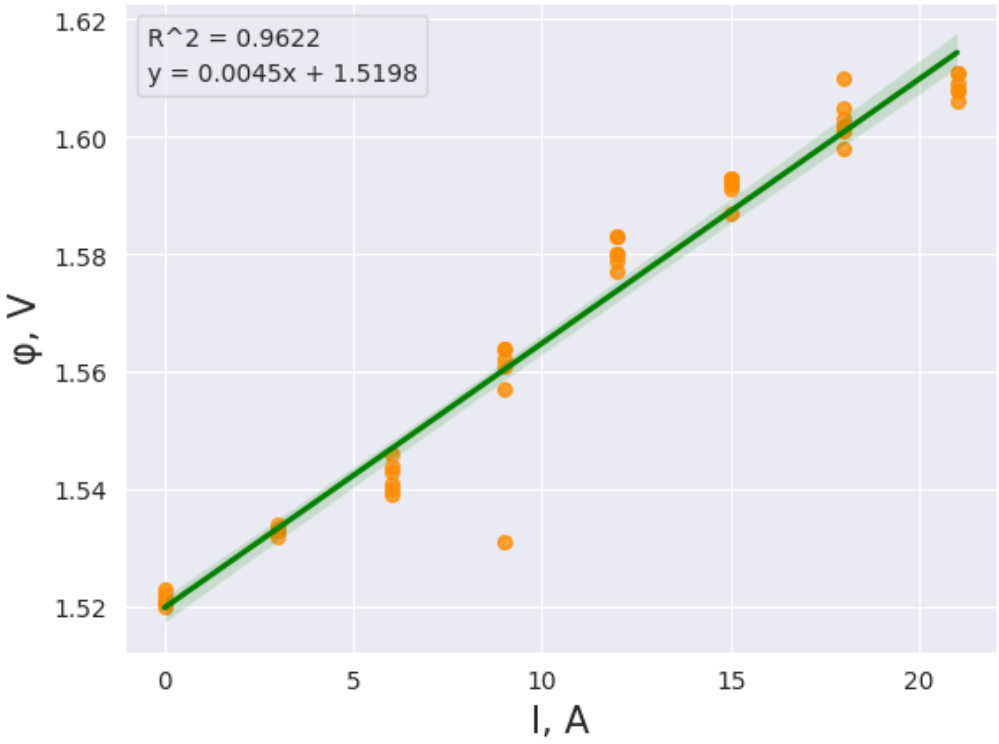

Figure 6: **Plot of the impact of the 371 km CPS on the protective potential difference at the 360 km CPS drainage baseline**

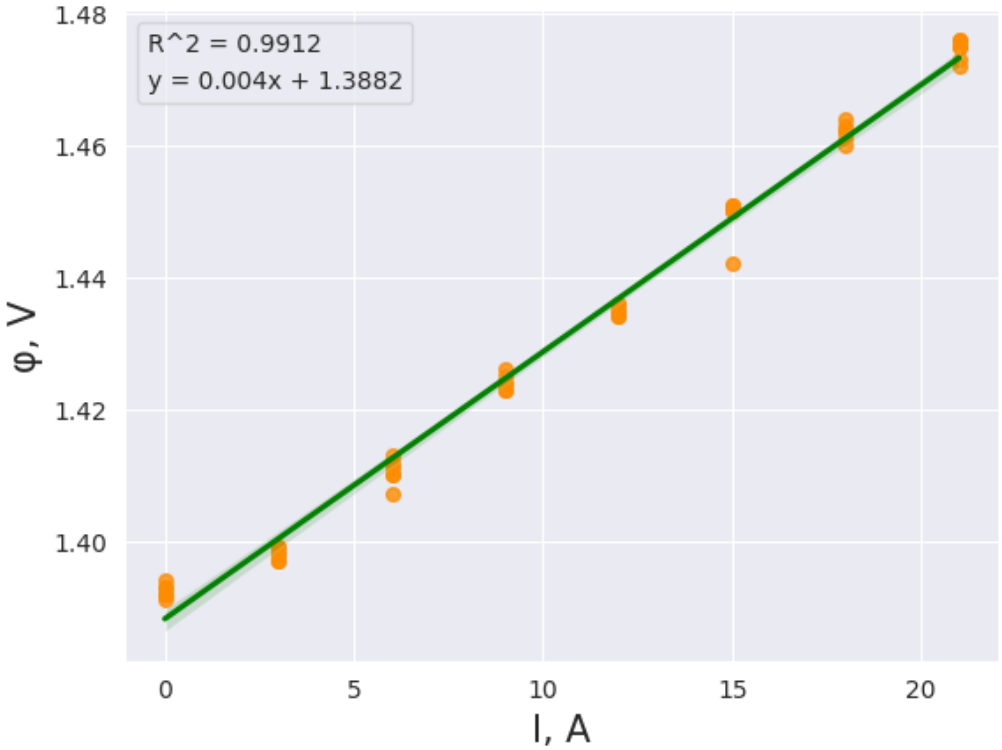

Figure 7: **Plot of the impact of the 384 km CPS on the protective potential difference at the 360 km CPS drainage baseline**

Based on the models developed above, the linear regression equations for the CPS of the pipeline section in question are as follows:

- CPS at 360 km:

$$\varphi = 0.2097 \cdot I + 1.2357 \quad (3.3.1.5)$$

- CPS at 336 km:

$$\varphi = 0.0032 \cdot I + 1.1879 \quad (3.3.1.6)$$

- CPS at 345 km:

$$\varphi = 0.0124 \cdot I + 1.7019 \quad (3.3.1.7)$$

- CPS at 371 km:

$$\varphi = 0.0045 \cdot I + 1.5198 \quad (3.3.1.8)$$

- CPS at 384 km:

$$\varphi = 0.004 \cdot I + 1.3882 \quad (3.3.1.9)$$

3.3.2 Improvement of CPS performance through the use of an elastomeric extended anode grounding

The calculation of the basic electrical characteristics of anode grounding is based on the normative document[7]. The input data for the calculation of the anode earthing characteristics are given in Table 3.

Parameter	Value
Specific resistance of the conductor material, Ohm·mm^2/m	0.018
Cross-sectional area of the conductor, mm^2	50
Specific electrical resistance of the electrode material – elastomer, Ohm·m	0.5
Electrode diameter, m	0.038
Current conductor diameter, m	0.018
Depth of anode ground electrode, m	1
Maximum protective potential of the pipeline, V	-2.5
Minimum protective potential of the pipeline, V	-0.9

[7] *RD 106-05. Rules for use of elastomeric anode grounding electrodes in cathodic protection installations and protective earthing circuits.*, 2005

Magnitude of the neutral potential of the pipeline, V	-0.55
Distance from gas pipeline surface to electrode, m	0.5
Specific resistance of copper wires, Ohm·m	0.018
Total length of connecting wires, m	500
Cross-sectional area of connecting wires, mm^2	300
Specific weight of the conductive rubber of the extended ground electrode, tn/m^3	1.35

Table 3: Input data

1. One of the main features used in the calculation of the parameters and operating modes of the CPS with extended anode grounding electrodes is the current propagation constant:

$$\alpha_{\mathrm{A}} = \sqrt{\frac{r_A}{R_A}}, \qquad (3.3.2.1)$$

r_A – longitudinal resistance of the extended electrode, Ohm/m (3.3.2.2);

R_A – transient resistance, Ohm·m (3.3.2.3).

2. Longitudinal resistance of the extended electrode:

$$r_A = \frac{\rho_{con}}{S_{con}}, \qquad (3.3.2.2)$$

ρ_{con} – specific resistance of the conductor material, Ohm·mm^2/m;

S_{con} – cross-sectional area of the conductor, mm^2

3. The transient resistance of an extended anode grounding electrode is determined as follows:

$$R_A = R_{TR} + R_{FR}, \qquad (3.3.2.3)$$

R_{TR} – transverse resistance of the electrode, Ohm·m (3.3.2.4);

R_{FR} – electrode current flow resistance, Ohm·m (3.3.2.5).

4. Transverse resistance of the electrode:

$$R_{TR} = \frac{\rho_{\mathrm{A}}}{\pi} \ln \frac{d_{\mathrm{A}}}{d_{\mathrm{T}}}, \qquad (3.3.2.4)$$

ρ_{A} – specific electrical resistance of the electrode material – elastomer, Ohm·m;

d_{A} – electrode diameter, m

d_{con} – current conductor diameter, m

5. Electrode current flow resistance:

$$R_{FR} = \frac{\rho_{\text{gr}}}{\pi} \ln \frac{1{,}12\sqrt{R_{FR}}}{\sqrt{r_{\text{A}} d_{\text{A}} H}}, \quad (3.3.2.5)$$

ρ_{gr} – the average electrical resistivity of the ground, Ohm·m;

H – depth of anode ground electrode, m

Since this equation is transcendental, the solution of the equation of determining the resistance of the electrode current flow resistance is done with software (in this case, with MathCAD).

6. Input resistance of the anode grounding electrode:

$$Z_{\text{A}} = k_z \sqrt{r_A R_A} \cdot \text{cth}(\alpha_{\text{A}} \cdot k_z \cdot L_{\text{A}}), \quad (3.3.2.6)$$

k_z – the construction constant of the CPS (k_z=1, for cantilevered asymmetrical anode connection scheme; k_z = 0.5 – for symmetrical anode connection scheme);

L_{A} – optimum length of extended anode grounding, m (3.3.2.7).

7. The optimum length of the extended anode grounding can be found as follows:

$$L_{\text{A}} = \frac{1}{\alpha_{\text{A}} \cdot k_z} \cdot \text{Arch} \frac{\Delta\varphi_0}{\Delta\varphi_m}, \quad (3.3.2.7)$$

$\text{Arch} \frac{\Delta\varphi_0}{\Delta\varphi_m} \approx 2{,}4$ at the regulated[8] values of the minimum required $\Delta\varphi_m$ and maximum permissible $\Delta\varphi_0$ shifts of the potential difference in the pipe-soil system.

8. Use a similar formula to calculate the protective zone of the anode grounding:

$$L_z = \frac{1}{\alpha_{\text{C}} \cdot k_z} \cdot \text{Arch} \frac{\Delta\varphi_0}{\Delta\varphi_m}, \quad (3.3.2.8)$$

α_{C} – current propagation constant in the “anode-pipeline” system (3.3.2.9)

9. Current propagation constant in the “anode-pipeline” system:

$$\alpha_{\text{C}} = \sqrt{\alpha_p \alpha_{\text{A}}}, \quad (3.3.2.9)$$

[8] *State Standard GOST R 51164-98 Steel pipe mains. General requirements for corrosion protection - Introduced 1999–07–01*, 1999

α_{T} – Current propagation constant along the gas pipeline (3.3.5).

10. Input resistance of the “anode-pipeline” system, Ohm:

$$Z_{\mathrm{C}} = Z_{\mathrm{A}} + Z_{\mathrm{p}}, \quad (3.3.2.10)$$

Z_{p} – pipeline inlet resistance, ohm (3.3.6).

11. Total anode grounding protection current:

$$I_A = \frac{\Delta\varphi_0}{\alpha_{\mathrm{C}} \cdot R_{\mathrm{t}}}, \quad (3.3.2.11)$$

R_{t} – the transient resistance of the pipeline, Ohm/m (3.3.4)

12. Maximum permissible potential difference displacement in “pipeline-ground” system:

$$\Delta\varphi_0 = |\varphi_{max}| - |\varphi_e|, \quad (3.3.2.12)$$

$|\varphi_{max}|$ – maximum protective potential of the pipeline, V;

$|\varphi_e|$ – the value of the neutral potential of the pipeline, V.

13. Ground resistance between the pipeline and the extended anode grounding electrode (value of current flow resistance in CPS) (at a≤5):

$$\mathrm{R}_{GR} = \kappa_{\mathrm{C}}^{*} \frac{\rho_{\mathrm{gr}}}{\pi \mathrm{L}_{\mathrm{A}}} \ln \frac{\mathrm{a}}{\sqrt{\mathrm{d}_{\mathrm{A}} \mathrm{d}_c}}, \quad (3.3.2.13)$$

H_p– depth of pipeline, m;

d_c – equivalent diameter of coke backfill, $\mathrm{d}_c = 3\sqrt{d_A} = 0.59\ m$;

a – distance from the surface of the gas pipeline to the anode grounding electrode, m;

k_{C}^{*} – coefficient of possible non-uniformity between the length of the pipe section to be protected and the anode earth electrode of the extended type:

$$k_{\mathrm{C}}^{*} = \sqrt{\frac{L_3}{L_{\mathrm{z}}}} \quad (3.3.2.14)$$

14. Output voltage from the CPS, V:

$$U_{\mathrm{CPS}} = I_A \cdot (Z_{\mathrm{c}} + R_{GR} + R_{\mathrm{d}}), \quad (3.3.2.15)$$

R_{d} – resistance of the drain line connecting the CPS to the anode grounding electrode, Ohm.

15. Resistance of the drain line connecting the CPS to the anode grounding:

$$R_{\text{d}} = \rho_{\text{w}} \frac{l_{\text{w}}}{S_{\text{w}}}, \qquad (3.3.2.16)$$

ρ_{w} – specific resistance of copper wires, $\rho_{\text{w}} = 0{,}018 \ \frac{Ohm \cdot mm^2}{m}$;

l_{w} – total length of connecting wires, l_{w} = 500 m;

S_{w} – cross-sectional area of connecting wires, $S_{\text{пр}}$ = 300 mm^2.

16. The power output of the CPS is determined by the following formula:

$$P_{\text{CPS}} = k_w \cdot U_{\text{CPS}} \cdot I_A, \qquad (3.3.2.17)$$

k_w – power reserve factor assumed for the CPS at the time of calculation, k_w=1.5.

17. The lifetime of the extended anode grounding is calculated as follows (extended anode grounding must have a lifetime of at least 50 years[9]):

$$T = \frac{G \cdot k}{q \cdot J(0) \cdot k_{\text{г}}}, \qquad (3.3.2.18)$$

G – specific mass of conductive rubber of the extended earth electrode, kg/m (3.3.2.19);

k – safety factor ($k = 0.8$);

q – electrochemical equivalent of anode material, $q = 0.25 \ {}^{kg}/_{\text{A} \cdot year}$.

$J(0)$ – linear anode current density at drainage point, A/m (3.3.2.20);

k_{gr} – coefficient of heterogeneity of the ground along the length of the anode (2.3.2.21).

$$G = \left(\frac{\pi d_A^2}{4} - S_w \cdot 10^{-6} \right) \cdot \gamma_r \cdot 10^3, \qquad (3.3.2.19)$$

γ_r – specific gravity of conductive rubber, tn/m^3.

$$J(0) = \alpha_{\text{A}} I_{A(avr)} \operatorname{cth}(\alpha_{\text{A}} \cdot I_A). \qquad (3.3.2.20)$$

$$k_{gr} = \frac{\rho_{gr(avr)}}{\rho_{gr(min)}}, \qquad (3.3.2.21)$$

[9] *RD 106-05. Rules for use of elastomeric anode grounding electrodes in cathodic protection installations and protective earthing circuits.*, 2005

$\rho_{gr(min)}$ – minimum electrical resistivity of the ground at the anode site, Ohm·m.

The results of the calculation of the main electrical characteristics of the extended anode grounding are shown in the Table 4.

№ section / **Parameter**	**1**	**2**	**3**	**4**	**5**
Longitudinal resistance of the extended electrode, Ohm/m	0.00036				
Transverse resistance of the electrode, Ohm·m	0.12				
Electrode current flow resistance, Ohm·m	113.68	133.31	124.61	141.68	122.77
The transient resistance of an extended anode grounding electrode, Ohm·m	113.80	133.43	124.73	141.80	122.89
Current propagation constant, 1/m	0.00178	0.00164	0.00170	0.00159	0.00171
Optimum length of the extended anode grounding, m	1349.36	1461.12	1412.68	1506.25	1402.22
Input resistance of the anode grounding electrode, Ohm	0.206	0.223	0.215	0.230	0.214
Current propagation constant in the “anode-pipeline” system, 1/m	0.00042	0.00040	0.00041	0.00040	0.00041
Protective zone of the anode grounding, m	9534.63	15049.85	11097.28	13036.42	9495.45
Input resistance of the “anode-pipeline” system, Ohm	0.251	0.259	0.256	0.268	0.284
Maximum permissible potential difference displacement in “pipeline-ground” system, V	1.95				
Total anode grounding protection current, A	6.94	9.15	7.06	8.23	7.04
Coefficient of possible non-uniformity of the length of the pipe section to be protected	2.66	3.21	2.80	2.94	2.60
Ground resistance between the pipeline and the extended anode grounding electrode, Ohm	0.033	0.043	0.037	0.041	0.034
Resistance of the drain line connecting the CPS to the anode grounding, Ohm	0.03				
Output voltage from the CPS, V	1.775	3.041	2.280	2.787	2.452
The power output of the CPS, W	18.487	41.733	24.159	34.406	25.910
Specific mass of conductive rubber of the extended earth electrode, kg/m	40.22				

Linear anode current density at drainage point, A/m	1.107	0.840	1.88	0.934	1.091
Coefficient of heterogeneity of the ground along the length of the anode	1.1112				
The lifetime of the extended anode grounding, years	104.643	137.891	106.438	124.029	106.149

Table 4: Calculated electrical characteristics of anode grounding

3.4 Results

The coefficient of determination R^2, which assesses the validity of the model proposed in Section 3.3.1 of this paper, is as follows:

- CPS at 360 km: $R^2 = 0.9991$
- CPS at 336 km: $R^2 = 0.9734$
- CPS at 345 km: $R^2 = 0.9816$
- CPS at 371 km: $R^2 = 0.9622$
- CPS at 384 km: $R^2 = 0.9912$.

The values in this work are less accurate compared to the calculated values of the determination coefficients presented in the work of S.A. Nikulin. Perhaps, the high accuracy of the model presented in (Nikulin, 2015) is due to the fact that the authors conducted their experiments under different laying conditions: in the middle zone, there is loess, whereas in this work the calculations were performed on the study object located in the circumpolar zone, where there are many bogs and the soil is formed by peatlands. In addition, there may be a small number of unknown external current sources affecting the pipeline to be protected, as well as a large number of rivers and lakes along the pipeline route.

The value of the external potential is calculated using equation (3.2.5). According to the obtained linear regression equation model (3.3.1.5 – 3.3.1.9), the coefficient of influence of the n^{th} effective value on the total potential difference at the measurement point takes the following values:

- CPS at 360 km: $A_{11} = 0.2097$
- CPS at 336 km: $A_{12} = 0.0032$
- CPS at 345 km: $A_{13} = 0.0124$

- CPS at 371 km: A_{14} = 0.0045
- CPS at 384 km: A_{15} = 0.004.

Consequently, equation (3.2.5) will take the following form:

$$\varphi_{external} = \varphi_1 - 0.2097 \cdot I_1 - 0.0032 \cdot I_2 - 0.0124 \cdot I_3 - 0.0045 \cdot I_4 - 0.004 \cdot I_5$$

The external potential equation obtained provides the opportunity to subsequently optimise the operating mode of the CPS by modelling the total protection potential distribution on the main gas pipe. In this case, when solving the optimisation problem, the external potential allows the CPS to be disconnected for only a short period of time in order to establish the influence coefficients for each CPS, on the basis of which further calculations can be carried out, rather than the potential of the pipe itself.

№ of the experiment		1	2	3	4	5	6
№	*I, A*	φ, V					
1	0	1.2357	1.2357	1.2357	1.2357	1.2357	1.2357
2	1	1.4454	1.4454	1.4454	1.4454	1.4454	1.4454
3	2	1.6551	1.6551	1.6551	1.6551	1.6551	1.6551
4	3	1.8648	1.8648	1.8648	1.8648	1.8648	1.8648
5	4	2.0745	2.0745	2.0745	2.0745	2.0745	2.0745
6	5	2.2842	2.2842	2.2842	2.2842	2.2842	2.2842
7	6	2.4939	2.4939	2.4939	2.4939	2.4939	2.4939
8	7	2.7036	2.7036	2.7036	2.7036	2.7036	2.7036
9	8	2.9133	2.9133	2.9133	2.9133	2.9133	2.9133
10	9	3.123	3.123	3.123	3.123	3.123	3.123
11	10	3.3327	3.3327	3.3327	3.3327	3.3327	3.3327
12	11	3.5424	3.5424	3.5424	3.5424	3.5424	3.5424
13	12	3.7521	3.7521	3.7521	3.7521	3.7521	3.7521
14	13	3.9618	3.9618	3.9618	3.9618	3.9618	3.9618

Table 5: Calculated values of protective potential by linear approximation at the drainage point of the central CPS

Calculation of the relative error of the calculation of the protective potential difference at the drainage point of the 360 km central CPS is made according to the following formula:

$$\varepsilon_{\varphi} = \frac{\varphi_{\text{measured}} - \varphi_{\text{calculated}}}{\varphi_{\text{measured}}} \cdot 100\% \qquad (3.4.1)$$

№	№ of the experiment						Average
	1	2	3	4	5	6	
1	0.30%	0.31%	0.30%	0.29%	0.29%	0.27%	0.29%
2	2.00%	1.99%	2.00%	1.74%	2.00%	1.95%	1.95%
3	1.40%	0.92%	1.41%	1.48%	1.48%	1.42%	1.35%
4	1.09%	0.97%	0.95%	1.02%	0.96%	0.98%	0.99%
5	1.36%	1.33%	1.31%	1.32%	1.35%	1.31%	1.33%
6	0.85%	0.85%	0.84%	0.84%	0.86%	1.29%	0.92%
7	0.24%	0.24%	0.24%	0.24%	0.25%	0.25%	0.24%
8	1.64%	1.64%	1.65%	1.65%	1.65%	1.65%	1.65%
9	0.56%	0.18%	0.35%	0.39%	0.53%	0.18%	0.37%
10	1.80%	1.95%	1.93%	2.01%	1.99%	1.84%	1.92%
11	0.62%	0.48%	0.62%	0.61%	0.63%	0.62%	0.60%
12	0.14%	0.14%	0.14%	0.18%	0.13%	0.13%	0.14%
13	0.01%	0.01%	0.02%	0.00%	0.01%	0.18%	0.04%
14	0.49%	0.49%	0.49%	0.49%	0.50%	0.50%	0.49%

Table 6: Errors in calculating the potential at the drainage point

For the subsequent applications of the obtained data, it is not sufficient to assess the adequacy of the model, as the coefficients of determination provide more of an estimate of the accuracy of the obtained model, but do not confirm its validity.

One of the basic assumptions of linear regression is that there is no correlation between successive residuals. In other words, it assumes that the residuals are independent. The residuals are the difference between the observed and predicted values in a regression analysis.

Regression error autocorrelation is the correlation between random regression errors in different observations (Dougherty, 2011).

In practice, error autocorrelation manifests itself in the behaviour of the regression residuals:

$$e_i = y_i - \widehat{y_i}, \qquad (3.4.2)$$

y – the observed value (response);

$\widehat{y_i}$ – calculated value ($\hat{y} = \alpha + \beta x$).

The presence of regression residuals indicates that they do not have the lowest variance of all linear unbiased estimates, which makes the estimates of regression parameters obtained by the ordinary least squares method inefficient, although they can also be used for interpretation and prediction. More dangerously, however, when the residuals are correlated, the standard errors of the regression parameter estimates become untenable and so cannot be used to construct confidence intervals for these estimates, nor can Student's t-test be used to test hypotheses about their significance (Bazilevsky, 2018).

When the assumption that the estimates are independent is violated, the standard errors of the coefficients in the regression model are likely to be underestimated, meaning that the predictor variables are more likely to be considered statistically significant, when in fact they are not.

If the sample regression satisfactorily describes the true relationship between y and x, then the residual e_i should be an independent normally distributed random variable with a mean of zero and there should be no trend in the value of e_i (Kobzar, 2006).

In order to obtain a more adequate regression equation and statistically non-differentiated calculations, it is recommended that the Durbin-Watson serial correlation coefficient be used:

$$DW = \frac{\sum_{t=2}^{n}(e_t - e_{t-1})^2}{\sum_{t=1}^{n} e_t^2} \qquad (2.4.3)$$

To determine the hypothesis that the residuals are correlated, the calculated coefficients are compared with the critical values DW_1 and DW_2 (Kobzar, 2006):

- If $DW < DW_1(\alpha)$ or $DW > 4\text{-}DW_1(\alpha)$, accept the hypothesis of a positive or negative correlation with confidence α, respectively;
- If $DW_2(\alpha) > DW > DW_1(\alpha)$ or $4\text{-}DW_1(\alpha) > DW > 4\text{-}DW_2(\alpha)$, the test does not allow the choice between the presence or absence of the residual correlation hypothesis;
- If $DW_2(\alpha) < DW < 4\text{-}DW_2(\alpha)$, then the hypothesis of correlation is rejected.

According to the reference data in (Kobzar, 2006), with a confidence level α = 0.95, the number of regression coefficients in the model k = 1 and the number of experiments performed n = 6, the critical value of the correlation coefficient is considered to be equal to:

- $DW_1(0.95) = 0.61$
- $DW_2(0.95) = 1.4$

To fully evaluate the model, regression residuals were calculated for each of the six experiments (3.4.2), followed by Durbin-Watson series correlation coefficients based on the data in the Annex tables 1-5 (Figures 8-12) the Python language package “Statsmodels” for statistical calculations, including descriptive statistics, estimation and statistical model output, was used to calculate Durbin-Watson coefficients. The class “durbin_watson” included in the package “statsmodels.stats.stattools” allows the exact calculation of serial correlation coefficients.

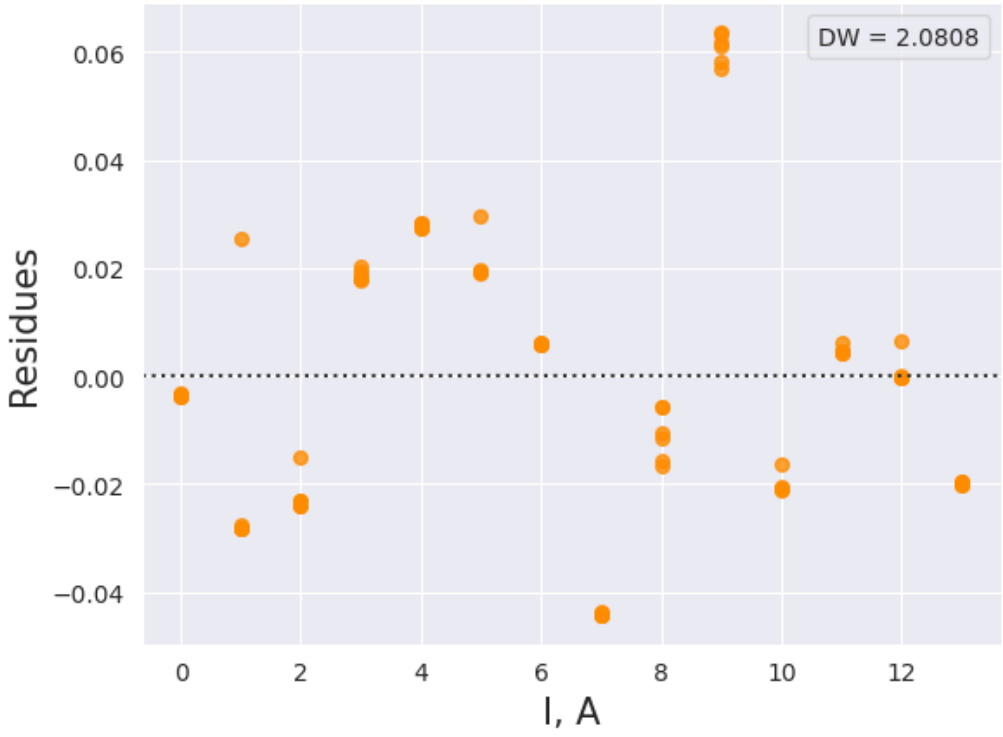

Figure 8: Regression residuals plot at different current strengths when adjusting the CPS at 360 km

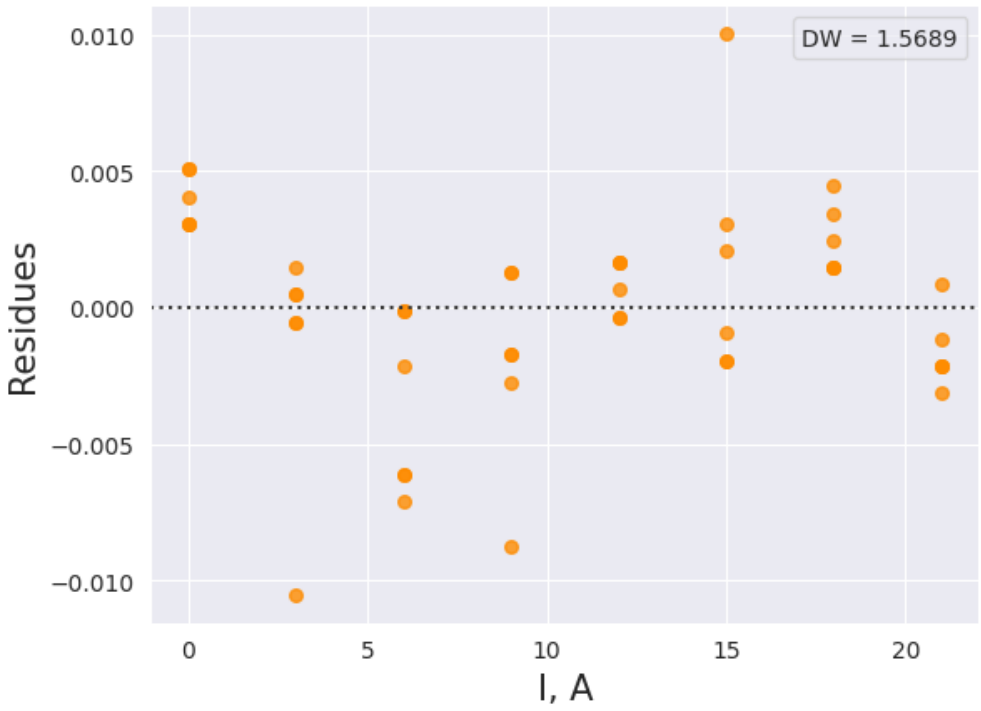

Figure 9: **Regression residuals plot at different current strengths when adjusting the CPS at 336 km**

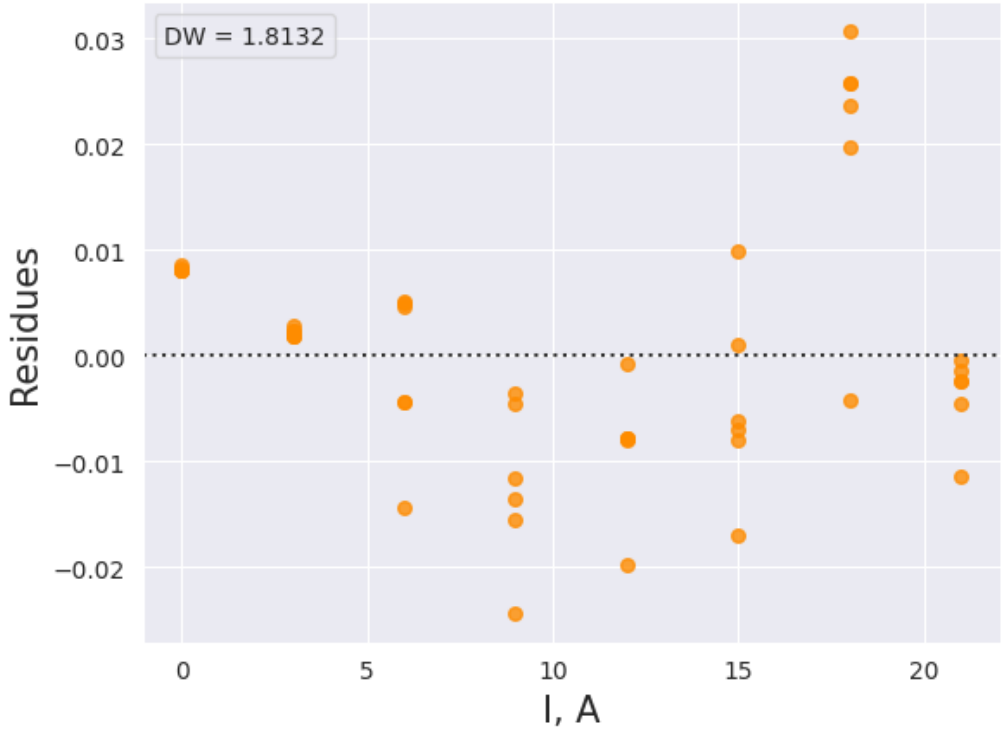

Figure 10: **Regression residuals plot at different current strengths when adjusting the CPS at 345 km**

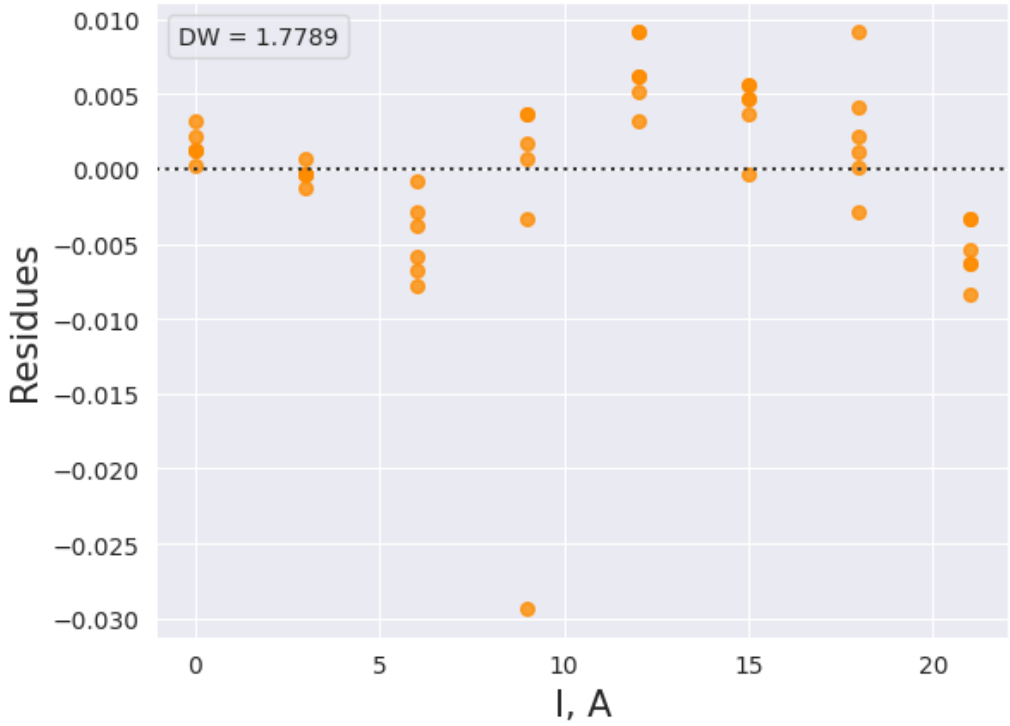

Figure 11: **Regression residuals plot at different current strengths when adjusting the CPS at 371 km**

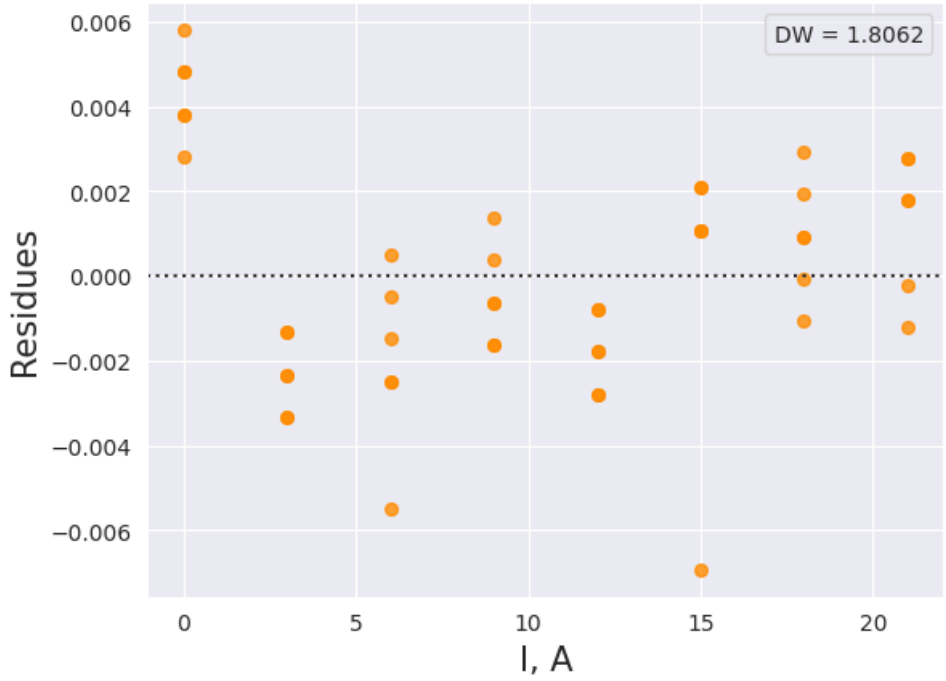

Figure 12: **Regression residuals plot at different current strengths when adjusting the CPS at 384 km**

Figure 13 shows the reference values for the Durbin-Watson coefficients (shown in green) and the calculated coefficient values for each CPS.

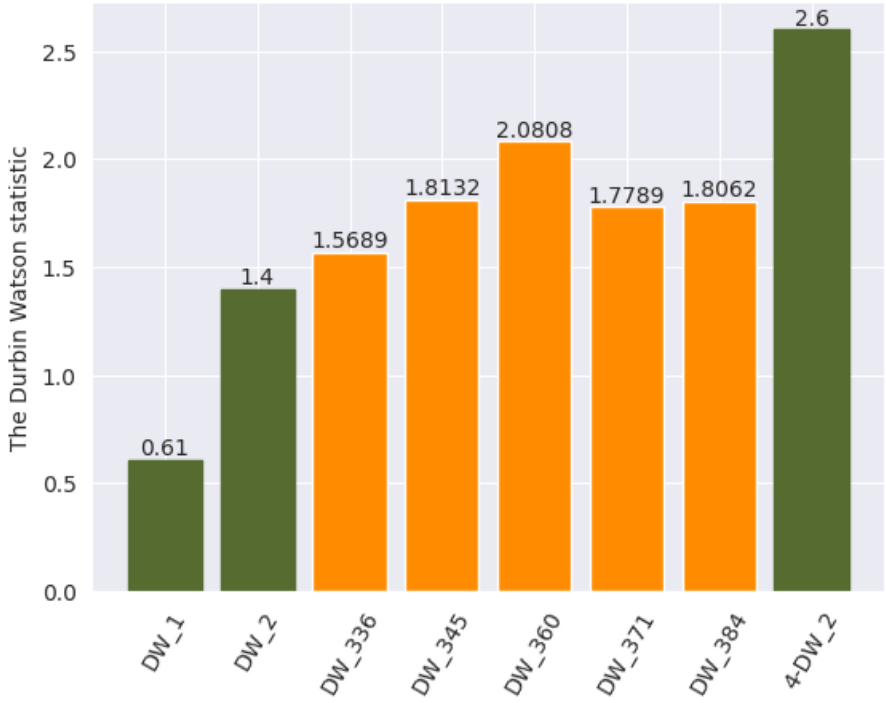

Figure 13: Values of the Durbin-Watson correlation coefficients in the given critical value interval

Since the calculated values satisfy the condition:

$$DW_2(\alpha) < DW < 4\text{-}DW_2(\alpha), \qquad (2.4.4)$$

then the resulting regression equations should be considered valid.

Furthermore, in order to analyse the effectiveness of the flexible anode earthing electrode, Table 7 presents a comparison of the power output of the CPS when using the existing grounding anodes and the elastomeric grounding anodes. The replacement of the grounding anode electrode is therefore justified, as this operation leads to a reduction in energy consumption and thus to a more efficient operation of the CPS.

	№ CPS					Total power, W	Absolute difference, W	Relative change, %
	1	2	3	4	5			
Power output of the CPS using the existing depth ground electrodes, W	42.342	73.982	48.801	56.662	38.456	260.243	115.548	44%

Power output of the CPS using the elastomeric ground electrodes, W	18.487	41.733	24.159	34.406	25.910	144.695		

Table 7: Comparison of power consumption when using different grounding anodes

4. Economic analysis

The process of optimisation of the cathodic protection station is a project whose product (i.e., result) is the derivation of a mathematical model of the distribution of the protection potential of a section of gas main pipeline, contributing to facilitating the procedure of optimal regulation of electrochemical protection system of the pipeline.

The practical application of this result is introduction of the received model to similar production objects – main gas pipelines with the same product pumping characteristics and media properties.

One of the methods used to assess advantages and disadvantages of the project is the application of a SWOT analysis.

SWOT analysis is a versatile strategic management technique. The object of SWOT analysis may be any product, company, shop, factory, country, educational institution or even a person.

SWOT analysis is a comprehensive analysis of a research project. SWOT analysis is used to investigate the external and internal environment of a project (Zub, 2023).

SWOT represents the following:

1. Strengths;
2. Weaknesses;
3. Opportunities;
4. Threats.

Table 8 presents the SWOT analysis for the project to improve the electrochemical protection performance of the linear sections of major gas pipelines.

Strengths:	**Weaknesses**:
• Cost-effectiveness and energy efficiency of the methodology; • Environmental feasibility of optimising the operation of the CPS; • Economic feasibility of the methodology.	• Lack of a prototype scientific design; • Lack of some input data affecting the validity of the methodology.
Opportunities:	**Threats**:
• Emergence of demand for the project implemented due to economic attractiveness.	• Introduction of additional customer specifications for the method model; • Introduction of additional national requirements regarding certification of the products used.

Table 8: SWOT analysis

Drafting the matrix entails breaking down the information into the following groups:

- **Strengths–Opportunities strategy** – the strengths and opportunities of the project are explored:

1. Develop a more effective method for identifying the sources of corrosion damage development during long-term operation of gas pipelines;
2. The continuation of scientific research to improve the method and its implementation in operational facilities.

- **Weaknesses–Opportunities strategy** – how to use opportunities to eliminate existing weaknesses:

1. Develop the concept of scientific research;
2. The acquisition of the necessary software and equipment.

- **Strengths–Threats strategy** – how strengths can be defended against uncontrollable external factors:

1. Promotion of new technologies to create demand.

- **Weaknesses–Threats strategy** – what activities are introduced to prevent future risks:

1. Developing the concept of scientific research;
2. Promotion of recommended methods and optimisation to create demand.

The application of third-party potential differences in the pipeline protective potential distribution model resulted in making it possible to determine the optimum parameters for the operation of the 336-384 km section of the “Punga-Ukhta-Gryazovets III” main gas pipeline without shutting down the CPS for a long period of time. This factor contributes to facilitate the optimum adjustment procedure for

the operation of the CPS. This is due to the fact that it is not necessary to disconnect all CPS simultaneously for a long period of time, up to a week. In this case it is sufficient to disconnect them sequentially to set the coefficients of influence of each CPS on the total protection potential difference.

The savings in the time required for measurement contribute to the fact that the pipeline does not need to be depolarised for a long period of time and hence is not exposed to stray currents on the insulation coating. The corrosive effects of stray currents accelerate the degradation of the protective coating, leading to additional costs for early replacement.

The second proposed method to optimise the operation of cathodic protection stations was to replace deep grounding electrodes with elastomeric extended anode grounding. The existing anode grounding electrodes in this section of the main gas pipeline are deep grounding electrodes.

The construction of deep anode grounding electrodes is several electrodes connected by a wire. Located at a depth of about 40 metres, they are coated with a coke mineral composition, which greatly increases the weight of the product. A drilling rig is used for installation, which makes the job more expensive. Despite the high cost, the range of deep anode grounding electrodes is increasing and their resistance is not dependent on the time of year.

When using long elastomeric anode ground electrodes, however, considerable savings can be made as this type of ground electrode is laid horizontally, usually in the same trench as the pipeline to be protected. Therefore, there is no need to drill holes for the installation of ground electrodes which reduces the installation costs compared to deep ground electrodes.

Feasibility calculations for anode grounding include determining optimum design parameters and number of anode electrodes to ensure minimum possible reduced total costs (in relation to one year of operation).

The speed of anode dissolution is very important as replacement of old grounding electrodes or premature failure of anode electrode not only incurs financial costs but can also lead to a catastrophe. The dissolution rate of a deep anode ground electrode is in the order of 0.5 kg/A- year. For extended anode earth electrodes

made of elastomeric materials of the ELER-2.1 series, the dissolution rate is 0.25 kg/A- year.

Extended anode ground electrodes are characterised by a reduced diffusion coefficient. In addition, during operation, the current density gradually evens out along the length of the anode, so the anode ground electrode is consumed evenly along its entire length, which contributes to a longer service life. The current density flowing from the anode cladding can also be controlled by the design of the anode. It is possible to manufacture the anode sheath with any declared characteristics, including variable conductivity in the radial direction and along the length of the anode. This is achieved by the use of cable technology in the manufacture of earth electrodes. This aspect is a key characteristic to ensure long and reliable performance of elastomeric earth electrodes (Delektorsky and Stefov, 2006).

An economic consequence of replacing anode earth electrodes is also a reduction in the power output of their CPS to drive current to the earth electrodes. Table 7 presented a comparison of the power output from the CPS when using existing anode grounding and elastomeric anode grounding. Thus, replacement of anode earth electrodes is justified, as this operation leads to a reduction of power consumption and therefore to a more efficient operation of the CPS, also from an economic point of view.

5. Environmental impact assessment

Transportation of hydrocarbons by pipeline remains the most efficient and safe way of transporting them over long distances. The reliability of the country's pipeline transport is largely determined by the good and serviceable condition of the main pipelines. One of the main aspects of pipelines deterioration is the corrosive effect of aggressive ground environment.

Corrosion cracking often becomes the reason of technical equipment failures and accidents, and as a result it leads to serious ecological consequences (Belvederesi and Dann, 2017; Ramírez-Camacho et al., 2017). Not only energy security of a state, but also ecological, social and economic development depends on failure-free and reliable operation of fuel and energy companies, gas pipeline transport facilities.

Therefore, pipeline condition monitoring, aimed at timely detection of corrosion damage as well as prevention of its development, is an important task.

As one of the suggested ways of increasing the efficiency of electrochemical protection, renewed anode earthing switches must meet the requirements of normative and technical documentation.

According to[10] anode grounding electrodes during operation should not cause adverse effects on the environment in amounts exceeding hygienic specifications specified in GOST 12.1.007-76 “Hazardous substances. Classification and general safety requirements”.

Also, during production of anode electrodes, control of maximum permissible emissions of harmful substances shall be carried out in accordance with GOST 17.2.3.02-2014 “Rules for Establishing Permissible Emissions of Pollutants by Industrial Enterprises”. Preliminary laboratory control of the level of harmful substances in the atmosphere shall be carried out according to the schedule agreed by the territorial authority of the Federal Office.

Depending on the degree of exposure anode earth electrodes belong to hazard category IV (low hazardous substances) according to GOST 12.1.007-76. Materials, used for making anode earthing switches must not release concentrations of products harmful for people and polluting environment under observance of conditions of their production, storage and operation.

Advantage of elastomeric earth electrodes as compared with deep ground electrodes is the higher environmental friendliness of their application. Elastomeric matrix has high elasticity, deformation elasticity and resistance to hydrogen, oxygen and other types of ageing as well as to corrosive media. The electrically conductive elastomer is chemically inert, which allows it to emit carbon dioxide when electrochemically attacking the carbon material, thus ensuring environmentally friendly operation of the anode grounding system.

[10] *State Standard GOST R 58344-2019 Earthing switches and grounding devices for various purposes. General technical requirements for anode grounding of electrochemical corrosion protection installations - Introduced 2019-06-01*, 2019

The proposed type of anode grounding is environmentally friendly, has low anode dissolution rate, does not contaminate water and process media with dissolution products.

The high flexibility and reliability of the current conductor contact assembly combined with environmental friendliness and the possibility to manufacture it as a “cable” with different sheath resistance make elastomeric anode earth electrodes indispensable for the protection of underground pipelines of any length.

6. Conclusion

Corrosion processes caused by the electrochemical interaction between the pipeline metal and the surrounding aggressive ground environment are the main cause of metal destruction or change of their properties, which constitutes a risk of gas pipelines depressurization, resulting in leakage of the transported hydrocarbon raw material and posing a threat to the life and health of operators and the surrounding communities.

An important aspect of maintaining the technical condition of the gas pipeline that meets regulatory requirements and corresponds to the efficient and reliable operation of hydrocarbon transportation is monitoring the corrosive impact on the pipeline metal, as well as preventing and minimising this impact. One of the main methods of pipeline protection against corrosion damage is electrochemical protection. For effective protection it is necessary to establish optimal operation of cathodic protection stations of pipelines. Optimization of parameters of electrochemical protection systems - definition of operation mode of CPS under which sufficient protection of a section of the gas main pipeline will be established and at that the total electric power spent on protection will be minimum.

The results of this work are:

1. An analysis of existing methodologies for the optimisation the operation of the CPS revealed that the most appropriate methodology is the one proposed by S.A. Nikulin (Nikulin et al., 2014; Nikulin, 2015). The method consists in determination of protective potential of a pipeline by means of suggested parameter – external potential, which takes into consideration influence of adjacent

CPS on protective potential in drainage point, as well as own potential of a pipeline. The advantage of this method is that there is no need to turn off all cathodic protection stations simultaneously for a long period of time for complete depolarisation of the pipeline. It is sufficient to switch off the CPS sequentially to establish the coefficients of influence of the CPS on the total potential difference.

2. By applying the method of mathematical statistics – regression analysis, a mathematical model of protective potential distribution for the section of “Punga-Ukhta-Gryazovets III” gas main pipeline has been developed. Coefficients of influence of each of 5 CPS (336 km, 345 km, 360 km, 371 km, 384 km) on the total potential difference are determined. The given coefficients contribute to facilitation of conducting optimal regulation of electrochemical protection system of the pipeline.

3. In order to check applicability of the method of regression analysis and adequacy of the obtained mathematical model, determination coefficients were calculated to estimate accuracy of the obtained model and Durbin-Watson serial coefficient to confirm reliability of the model.

Another method of increasing the efficiency of pipeline electrochemical protection system was the replacement of deep anode grounding electrodes with elastomeric extended anode grounding electrodes. Justification of this technological solution has been proved from technical-and-economical point of view as the analysis showed that this solution leads to saving of total power at CPS outlet by 44% in relation to existing operation modes of these stations, which is one of the key aspects of optimization of electrochemical protection system operation.

7. Bibliography

Aginey, R. V., Isupova, E. V., Alexandrov, O.Y., Alexandrov, Y. V., 2019. Patent No 2721250 C1 Russian Federation, IPC C23F 13/02. Method for determining the time of repair of anode grounding : No. 2019130420 : application. 25.09.2019 : publ. 18.05.2020.

Aginey, R. V., Isupova, E. V., Savchenkov, S. V., Yavorskaya, E.E., 2020. Patent No 2751713 C9 Russian Federation, IPC C23F 13/00. Method of anode grounding : No. 2020139836 : application. 02.12.2020 : publ. 07.09.2021.

Allahkaram, S.R., Isakhani-Zakaria, M., Derakhshani, M., Samadian, M., Sharifi-Rasaey, H., Razmjoo, A., 2015. Investigation on corrosion rate and a novel corrosion criterion for gas pipelines affected by dynamic stray current. J. Nat. Gas Sci. Eng. 26, 453–460. https://doi.org/10.1016/J.JNGSE.2015.06.044

Alvaro, A., Wan, D., Olden, V., Barnoush, A., 2019. Hydrogen enhanced fatigue crack growth rates in a ferritic Fe-3 wt%Si alloy and a X70 pipeline steel. Eng. Fract. Mech. 219. https://doi.org/10.1016/J.ENGFRACMECH.2019.106641

Artemenkov, V.Y., Koryakin, A.Y., Dikamov, D.V., Shustov, I.N., Shishkov, E.O., Yusupov, A.D., 2017. Organisation of corrosion monitoring at the facilities of the second section of the Achimovsky deposits in the Urengoy oil and gas condensate field. Gas Ind. J.

Bai, P. peng, Zhou, J., Luo, B. wei, Zheng, S. qi, Wang, P. yan, Tian, Y., 2020. Hydrogen embrittlement of X80 pipeline steel in H2S environment: Effect of hydrogen charging time, hydrogen-trapped state and hydrogen charging–releasing–recharging cycles. Int. J. Miner. Metall. Mater. 27, 63–73. https://doi.org/10.1007/S12613-019-1870-1

Bazilevsky, M.P., 2018. Research of New Criteria for Detecting First-order Residuals Autocorrelation in Regression Models. Math. Math. Model. 13–25. https://doi.org/10.24108/mathm.0318.0000102

Belvederesi, C., Dann, M.R., 2017. Statistical analysis of failure consequences for oil and gas pipelines. Int. J. Saf. Secur. Eng. 7, 103–112. https://doi.org/10.2495/SAFE-V7-N2-103-112

Ben Seghier, M.E.A., Höche, D., Zheludkevich, M., 2022. Prediction of the internal corrosion rate for oil and gas pipeline: Implementation of ensemble learning techniques. J. Nat. Gas Sci. Eng. 99, 104425. https://doi.org/10.1016/J.JNGSE.2022.104425

Benitez, J.L., Martinez, C., Roldan, R., 2002. Tests confirm effectiveness of new inhibitor for pipeline internal corrosion. Oil gas J. 100, 66–70.

Bertolini, L., Carsana, M., Pedeferri, P., 2007. Corrosion behaviour of steel in concrete in the presence of stray current. Corros. Sci. 49, 1056–1068. https://doi.org/10.1016/J.CORSCI.2006.05.048

Bolobov, V.I., Popov, G.G., Chernyshov, V.E., Usikov, D.V., 2022. Influence of various types of stresses on the intensity of corrosion processes in the pipeline steels. Научно-исследовательские публикации 24–27.

Bornukovskaya, K.A., Karnavskiy, E.L., Nikulin, S.A., Martynenko, S.A., 2019. Optimisation of the operation of electrochemical protection systems, depending on external factors and the current state of the gas pipeline. Neft. Territ. journalerritory jouranl.

Brenna, A., Beretta, S., Ormellese, M., 2020. AC Corrosion of Carbon Steel under Cathodic Protection Condition: Assessment, Criteria and Mechanism. A Review. Mater. 2020, Vol. 13, Page 2158 13, 2158. https://doi.org/10.3390/MA13092158

Brenna, A., Lazzari, L., Pedeferri, M., Ormellese, M., 2014. Cathodic protection condition in the presence of AC interference. La Metall. Ital. 6.

Broomfield, J.P., 2020. An overview of cathodic protection criteria for steel in atmospherically exposed concrete. Corros. Eng. Sci. Technol. 55, 303–310. https://doi.org/10.1080/1478422X.2020.1735715

Büchler, M., 2020. On the Mechanism of Cathodic Protection and Its Implications on Criteria Including AC and DC Interference Conditions. Corrosion 76, 451–463. https://doi.org/10.5006/3379

Cazenave, P., Jimenez, K., Gao, M., Moneta, A., Hryciuk, P., 2021. Hydrogen assisted cracking driven by cathodic protection operated at near −1200 mV CSE – an onshore natural gas pipeline failure. J. Pipeline Sci. Eng. 1, 100–121. https://doi.org/10.1016/J.JPSE.2021.02.002

Chatzidouros, E. V., Traidia, A., Devarapalli, R.S., Pantelis, D.I., Steriotis, T.A., Jouiad, M., 2019. Fracture toughness properties of HIC susceptible carbon steels in sour service conditions. Int. J. Hydrogen Energy 44, 22050–22063. https://doi.org/10.1016/j.ijhydene.2019.06.209

Chen, L., Du, Y., Liang, Y., Li, J., 2020. Research on corrosion behaviour of X65 pipeline steel under dynamic AC interference. https://doi.org/10.1080/1478422X.2020.1843819 56, 219–229. https://doi.org/10.1080/1478422X.2020.1843819

Chen, X., Li, X.G., Du, C.W., Cheng, Y.F., 2009. Effect of cathodic protection on corrosion of pipeline steel under disbonded coating. Corros. Sci. 51, 2242–2245. https://doi.org/10.1016/J.CORSCI.2009.05.027

Cheng, F., 2016. Monitor safety of aged fuel pipelines. Nat. 2016 5297585 529, 156–156. https://doi.org/10.1038/529156e

Cole, I.S., Marney, D., 2012. The science of pipe corrosion: A review of the literature on the corrosion of ferrous metals in soils. Corros. Sci. 56, 5–16. https://doi.org/10.1016/J.CORSCI.2011.12.001

Dann, M.R., Huyse, L., 2018. The effect of inspection sizing uncertainty on the maximum corrosion growth in pipelines. Struct. Saf. 70, 71–81. https://doi.org/10.1016/J.STRUSAFE.2017.10.005

Dann, M.R., Maes, M.A., 2018. Stochastic corrosion growth modeling for pipelines using mass inspection data. Reliab. Eng. Syst. Saf. 180, 245–254. https://doi.org/10.1016/J.RESS.2018.07.012

Delektorsky, A.A., Stefov, N.V., 2006. Features of elastomeric anodes. Neft. Territ. J. 34–37.

Devyaterikova, N., Nurmukhametova, M., Kharlashin, A., Popov, Y., 2019. Types of

corrosion damage of tubing in the oilfield. E3S Web Conf. 121. https://doi.org/10.1051/E3SCONF/201912103001

Dougherty, C., 2011. Introduction to econometrics, 4rd ed. Oxford University Press, Oxford.

Farh, H.M.H., Ben Seghier, M.E.A., Zayed, T., 2023. A comprehensive review of corrosion protection and control techniques for metallic pipelines. Eng. Fail. Anal. 143, 106885. https://doi.org/10.1016/J.ENGFAILANAL.2022.106885

Fatrakhmanov, F.K., 1998. The concept and ways to optimise cathodic protection of site communications. Sci. Tech. Collect. Mod. Probl. Gas Pipeline Transp. 408–411.

Folena, M.C., Ponciano, J.A. da C., 2020. Assessment of hydrogen embrittlement severity of an API 5LX80 steel in H2S environments by integrated methodologies. Eng. Fail. Anal. 111, 104380. https://doi.org/10.1016/J.ENGFAILANAL.2020.104380

Gan, L., Huang, F., Zhao, X., Liu, J., Cheng, Y.F., 2018. Hydrogen trapping and hydrogen induced cracking of welded X100 pipeline steel in H2S environments. Int. J. Hydrogen Energy 43, 2293–2306. https://doi.org/10.1016/J.IJHYDENE.2017.11.155

Ghosh, G., Rostron, P., Garg, R., Panday, A., 2018. Hydrogen induced cracking of pipeline and pressure vessel steels: A review. Eng. Fract. Mech. 199, 609–618. https://doi.org/10.1016/J.ENGFRACMECH.2018.06.018

Goidanich, S., Lazzari, L., Ormellese, M., 2010. AC corrosion. Part 2: Parameters influencing corrosion rate. Corros. Sci. 52, 916–922. https://doi.org/10.1016/J.CORSCI.2009.11.012

Goodwin, F.R., 2019. U.S. Patent no. 10,214,819 Galvanic anode and method of corrosion protection.

Gu, C., Hu, J., Zhong, X., 2020. The coating delamination mitigation of epoxy coatings by inhibiting the hydrogen evolution reaction. Prog. Org. Coatings 147, 105774. https://doi.org/10.1016/J.PORGCOAT.2020.105774

Hao, W., Liu, Z., Wu, W., Li, X., Du, C., Zhang, D., 2018. Electrochemical characterization and stress corrosion cracking of E690 high strength steel in wet-dry cyclic marine environments. Mater. Sci. Eng. A 710, 318–328. https://doi.org/10.1016/J.MSEA.2017.10.042

Kajiyama, F., 2008. JP. Patent no. JP2008096398A Cathode corrosion preventing system and cathode corrosion preventing method by galvanic anode system, pipeline soundness evaluating system and soundness evaluating method.

Kobzar, A.I., 2006. Applied Mathematical Statistics. For Engineers and Scientists. Fizmatlit, Moscow.

Kopytin, V.E., 2005. Features of calculating the parameters of cathodic protection with elastomeric electrodes of anode grounding of an extended type. Neft. Territ. J. 19–23.

Koyama, M., Akiyama, E., Lee, Y.K., Raabe, D., Tsuzaki, K., 2017. Overview of hydrogen embrittlement in high-Mn steels. Int. J. Hydrogen Energy 42, 12706–12723. https://doi.org/10.1016/j.ijhydene.2017.02.214

Kuang, D., Cheng, Y.F., 2016. Effects of alternating current interference on cathodic protection potential and its effectiveness for corrosion protection of pipelines. http://dx.doi.org/10.1080/1478422X.2016.1175773 52, 22–28. https://doi.org/10.1080/1478422X.2016.1175773

Kuang, D., Cheng, Y.F., 2015. Study of cathodic protection shielding under coating disbondment on pipelines. Corros. Sci. 99, 249–257. https://doi.org/10.1016/J.CORSCI.2015.07.012

Kumar Thakur, A., Kumar Arya, A., Sharma, P., 2021. Corrosion of pipe steels under alternating currents. Int. J. Electrochem. Sci 16, 211245. https://doi.org/10.20964/2021.12.22

Laureys, A., Depraetere, R., Cauwels, M., Depover, T., Hertelé, S., Verbeken, K., 2022. Use of existing steel pipeline infrastructure for gaseous hydrogen storage and transport: A review of factors affecting hydrogen induced degradation. J. Nat. Gas Sci. Eng. 101, 104534. https://doi.org/10.1016/J.JNGSE.2022.104534

Li, H., Niu, R., Li, W., Lu, H., Cairney, J., Chen, Y.S., 2022. Hydrogen in pipeline steels: Recent advances in characterization and embrittlement mitigation. J. Nat. Gas Sci. Eng. 105, 104709. https://doi.org/10.1016/J.JNGSE.2022.104709

Li, Y., Gong, B., Li, X., Deng, C., Wang, D., 2018. Specimen thickness effect on the property of hydrogen embrittlement in single edge notch tension testing of high strength pipeline steel. Int. J. Hydrogen Energy 43, 15575–15585. https://doi.org/10.1016/j.ijhydene.2018.06.118

Liang, Y., Du, Y., Zhu, Z., Chen, L., Liu, Y., Zhang, L., Qiao, L., 2023. Investigation on AC corrosion of aluminum alloy sacrificial anode in the artificial simulated seawater environment. Electrochim. Acta 446, 142002. https://doi.org/10.1016/J.ELECTACTA.2023.142002

Litvinenko, V., 2020. The role of hydrocarbons in the global energy agenda: The focus on liquefied natural gas. Resources 9. https://doi.org/10.3390/RESOURCES9050059

Liu, H., Liu, W., Wei, J., Liu, S., Dong, Z., 2023. Effect of stray current on corrosion behavior of Mg alloy sacrificial anode in buried pipeline. Eng. Fail. Anal. 143, 106852. https://doi.org/10.1016/J.ENGFAILANAL.2022.106852

Liu, Z.Y., Li, X.G., Cheng, Y.F., 2011. Effect of strain rate on cathodic reaction during stress corrosion cracking of X70 pipeline steel in a near-neutral pH solution. J. Mater. Eng. Perform. 20, 1242–1246. https://doi.org/10.1007/S11665-010-9770-6/METRICS

Lynch, S., 2012. Hydrogen embrittlement phenomena and mechanisms. Corros. Rev. 30, 105–123. https://doi.org/10.1515/corrrev-2012-0502

Lyubchik, A.N., Krapivskii, E.I., Bol'shunova, O.M., 2011. Prediction of the technical status of pipeline based on analysis. J. Min. Inst. 192, 153.

Mahdavi, F., Forsyth, M., Tan, M.Y.J., 2017. Understanding the effects of applied cathodic protection potential and environmental conditions on the rate of cathodic disbondment of coatings by means of local electrochemical measurements on a multi-electrode array. Prog. Org. Coatings 103, 83–92. https://doi.org/10.1016/J.PORGCOAT.2016.10.020

Mahdavi, F., Tan, M.Y.J., Forsyth, M., 2015. Electrochemical impedance

spectroscopy as a tool to measure cathodic disbondment on coated steel surfaces: Capabilities and limitations. Prog. Org. Coatings 88, 23–31. https://doi.org/10.1016/J.PORGCOAT.2015.06.010

Makarenko, V.D., 2009. Fundamentals of Corrosion Failure of Pipelines: Textbook. A Tyumen industrial University, Tyumen.

Medvedeva, M.L., Muradov, A.V., Prygaev, A.K., 2013. Corrosion and protection of main pipelines and tanks. National University of Oil and Gas «Gubkin University».

Mohammed, S.A.H., Abdulbaqi, I.M., 2018. Numerical Study and Design of an Impressed Current Cathodic Protection System for Buried Metallic Pipes. 2018 3rd Sci. Conf. Electr. Eng. SCEE 2018 95–100. https://doi.org/10.1109/SCEE.2018.8684076

Mohtadi-Bonab, M.A., Masoumi, M., Szpunar, J.A., 2021. A comparative fracture analysis on as-received and electrochemically hydrogen charged API X60 and API X60SS pipeline steels subjected to tensile testing. Eng. Fail. Anal. 129, 105721. https://doi.org/10.1016/J.ENGFAILANAL.2021.105721

Mohtadi-Bonab, M.A., Szpunar, J.A., Razavi-Tousi, S.S., 2013. A comparative study of hydrogen induced cracking behavior in API 5L X60 and X70 pipeline steels. Eng. Fail. Anal. 33, 163–175. https://doi.org/10.1016/J.ENGFAILANAL.2013.04.028

Nagumo, M., 2016. Fundamentals of hydrogen embrittlement. Fundam. Hydrog. Embrittlement 1–239. https://doi.org/10.1007/978-981-10-0161-1

Nagumo, M., Takai, K., 2019. The predominant role of strain-induced vacancies in hydrogen embrittlement of steels : Overview. Acta Mater. 722–733. https://doi.org/10.1016/j.actamat.2018.12.013

Nanninga, N., Slifka, A., Levy, Y., White, C., 2010. A Review of Fatigue Crack Growth for Pipeline Steels Exposed to Hydrogen. J. Res. Natl. Inst. Stand. Technol. 115, 437. https://doi.org/10.6028/JRES.115.030

Nikulin, A.S., Aginey, V.R., Karnavskiy, L.E., 2014. Improving the methodology for optimising the electrochemical protection of trunk pipelines. J. Pipeline Transp. Theory Pract. 10–14.

Nikulin, S.A., 2015. ncrease of Efficiency Prevention of Corrosion on Oil and Gas Pipelines on the Basis of Optimum Regulation of Working Modes of Cathodic Protection Stations: Cand. Sci. (Eng.) Dissertation. Ukhta.

Nykyforchyn, H., Tsyrulnyk, O., Zvirko, O., Krechkovska, H., 2019. Non-destructive evaluation of brittle fracture resistance of operated gas pipeline steel using electrochemical fracture surface analysis. Eng. Fail. Anal. 104, 617–625. https://doi.org/10.1016/J.ENGFAILANAL.2019.06.037

Nykyforchyn, H., Zvirko, O., Tsyrulnyk, O., Kret, N., 2017. Analysis and mechanical properties characterization of operated gas main elbow with hydrogen assisted large-scale delamination. Eng. Fail. Anal. 82, 364–377. https://doi.org/10.1016/J.ENGFAILANAL.2017.07.015

Odegov, V.E., Naumenko, D.B., Burma, V.V., 2019. Patent no. 193633 U1 Russian Federation, IPC C23F 13/16. Extended anode grounding: No. 2019119995 : application. 27.06.2019 : publ. 07.11.2019.

Ohaeri, E., Eduok, U., Szpunar, J., 2018. Hydrogen related degradation in pipeline

steel: A review. Int. J. Hydrogen Energy 43, 14584–14617. https://doi.org/10.1016/J.IJHYDENE.2018.06.064

Paul, D., 2016. DC Stray Current in Rail Transit Systems and Cathodic Protection. IEEE Ind. Appl. Mag. 22, 8–13. https://doi.org/10.1109/MIAS.2015.2481754

Politov, M.P., 2019. Patent No 2690581 C1 Russian Federation, IPC C23F 13/02, C23F 13/16. anode grounding : No 2018106954 : application. 29.02.2016 : publ. 04.06.2019.

Qian, S., Cheng, Y.F., 2017. Accelerated corrosion of pipeline steel and reduced cathodic protection effectiveness under direct current interference. Constr. Build. Mater. 148, 675–685. https://doi.org/10.1016/J.CONBUILDMAT.2017.05.024

Qin, G., Cheng, Y.F., 2021. A review on defect assessment of pipelines: Principles, numerical solutions, and applications. Int. J. Press. Vessel. Pip. 191, 104329. https://doi.org/10.1016/J.IJPVP.2021.104329

Qin, H., Du, Y., Lu, M., Sun, X., Zhang, Y., 2020. Experimental study on the corrosion behavior of X70 steel under asymmetric dynamic DC interference. Mater. Corros. 71, 1856–1871. https://doi.org/10.1002/MACO.202011725

Ramírez-Camacho, J.G., Carbone, F., Pastor, E., Bubbico, R., Casal, J., 2017. Assessing the consequences of pipeline accidents to support land-use planning. Saf. Sci. 97, 34–42. https://doi.org/10.1016/J.SSCI.2016.01.021

RD 106-05. Rules for use of elastomeric anode grounding electrodes in cathodic protection installations and protective earthing circuits., 2005. . VNIIGAZ, Moscow.

Rebrova, I.A., 2016. Theory of Experiment Planning. SibADI, Omsk.

Redekop, A.G., 2022. Patent No. 211707 U1 Russian Federation, IPC C23F 13/16. Extended anode of the electrochemical protection system for the underground facility : No. 2021137536 : application. 17.12.2021 : publ. 20.06.2022.

Robertson, I.M., Sofronis, P., Nagao, A., Martin, M.L., Wang, S., Gross, D.W., Nygren, K.E., 2014. Hydrogen Embrittlement Understood. Edward DeMille Campbell Meml. Lect. ASM Internatinal. https://doi.org/10.1007/s11661-015-2836-1

Ronevich, J.A., D'Elia, C.R., Hill, M.R., 2018. Fatigue crack growth rates of X100 steel welds in high pressure hydrogen gas considering residual stress effects. Eng. Fract. Mech. 194, 42–51. https://doi.org/10.1016/j.engfracmech.2018.02.030

Ruschau, G., Chen, Y., 2006. Determining the CP Shielding Behavior of Pipeline Coatings in the Laboratory. Corros. San Diego, Calif.

Schippl, V., Brück, S., Christ, H.J., Fritzen, C.P., Schwarz, M., Weihe, S., 2018. Modeling of hydrogen effects on short crack propagation in a metastable austenitic stainless steel (X2CrNi19-11). MATEC Web Conf. 165. https://doi.org/10.1051/MATECCONF/201816522005

Shaalan, E.M., Mostafa, M.A., Hamza, A.S., Al-Gabalawy, M., 2022. Cathodic Protection Performance Improvement of Metallic Pipelines based on Different DC Compensation Methods. Electr. Power Syst. Res. 210, 108064. https://doi.org/10.1016/J.EPSR.2022.108064

Shaposhnikov, N., Golubev, I., Khorobrov, S. V., Kolotiy, A.I., Ioffe, A. V., Revyakin, V.A., 2022. Autoclave modeling of corrosion processes occurring in a gas pipeline

during transportation of an unprepared multiphase medium containing CO2. J. Min. Inst. 258, 915–923. https://doi.org/10.31897/PMI.2022.92

Singh, R., Singh, A., Singh, P.K., Mahajan, D.K., 2019. Role of prior austenite grain boundaries in short fatigue crack growth in hydrogen charged RPV steel. Int. J. Press. Vessel. Pip. 171, 242–252. https://doi.org/10.1016/j.ijpvp.2019.03.004

Singh, V., Singh, R., Arora, K.S., Mahajan, D.K., 2019. Hydrogen induced blister cracking and mechanical failure in X65 pipeline steels. Int. J. Hydrogen Energy 44, 22039–22049. https://doi.org/10.1016/j.ijhydene.2019.06.098

Skuridin, N.N., Kuznetsov, A.A., Neganov, D.A., 2011. Determination of optimum operation modes of cathodic protection stations for the electrochemical protection system of main pipelines. Sci. Technol. Oil Oil Prod. Pipeline Transp. 90–94.

Solgaard, A.O.S., Carsana, M., Geiker, M.R., Küter, A., Bertolini, L., 2013. Experimental observations of stray current effects on steel fibres embedded in mortar. Corros. Sci. 74, 1–12. https://doi.org/10.1016/J.CORSCI.2013.03.014

State Standard GOST R 51164-98 Steel pipe mains. General requirements for corrosion protection - Introduced 1999–07–01, 1999. . Gosstandart of Russia, Moscow.

State Standard GOST R 58344-2019 Earthing switches and grounding devices for various purposes. General technical requirements for anode grounding of electrochemical corrosion protection installations - Introduced 2019-06-01, 2019. . Federal Agency for Technical Regulation and Metrology, Moscow.

Szeliga, M.J., 2012. Cathodic Protection of Ductile Iron and Steel Water Pipelines. Pipelines 2012 Innov. Des. Constr. Oper. Maint. - Doing More with Less - Proc. Pipelines 2012 Conf. 1176–1181. https://doi.org/10.1061/9780784412480.109

Tcvetkov, P., Cherepovitsyn, A., Makhovikov, A., 2020. Economic assessment of heat and power generation from small-scale liquefied natural gas in Russia. Energy Reports 6, 391–402. https://doi.org/10.1016/J.EGYR.2019.11.093

Teran, G., Capula-Colindres, S., Velázquez, J.C., Angeles-Herrera, D., Torres-Santillán, E., 2019. On the Influence of the Corrosion Defect Size in the Welding Bead, Heat-Affected Zone, and Base Metal in Pipeline Failure Pressure Estimation: A Finite Element Analysis Study. J. Press. Vessel Technol. Trans. ASME 141. https://doi.org/10.1115/1.4042908

Tian, H., Wang, X., Cui, Z., Lu, Q., Wang, L., Lei, L., Li, Y., Zhang, D., 2018. Electrochemical corrosion, hydrogen permeation and stress corrosion cracking behavior of E690 steel in thiosulfate-containing artificial seawater. Corros. Sci. 144, 145–162. https://doi.org/10.1016/J.CORSCI.2018.08.048

Traidia, A., Chatzidouros, E., Jouiad, M., 2018. Review of hydrogen-assisted cracking models for application to service lifetime prediction and challenges in the oil and gas industry. Corros. Rev. 36, 323–347. https://doi.org/10.1515/CORRREV-2017-0079/ASSET/GRAPHIC/J_CORRREV-2017-0079_FIG_006.JPG

Wan, H., Song, D., Li, X., Zhang, D., Gao, J., Du, C., 2017. Failure Mechanisms of the Coating/Metal Interface in Waterborne Coatings: The Effect of Bonding. Mater. 2017, Vol. 10, Page 397 10, 397. https://doi.org/10.3390/MA10040397

Wang, C., Li, W., Wang, Y., 2021a. Remaining lifetime assessment of gas pipelines subjected to stray current interference using an integrated electric-electrochemical

method. Eng. Fail. Anal. 127, 105494. https://doi.org/10.1016/J.ENGFAILANAL.2021.105494

Wang, C., Li, W., Wang, Y., 2021b. A probabilistic-based model for dynamic predicting pitting corrosion rate of pipeline under stray current interference. J. Pipeline Sci. Eng. 1, 339–348. https://doi.org/10.1016/J.JPSE.2021.09.003

Wang, C., Li, W., Wang, Y., Xu, S., Yang, X., 2019a. Chloride-induced stray current corrosion of Q235A steel and prediction model. Constr. Build. Mater. 219, 164–175. https://doi.org/10.1016/J.CONBUILDMAT.2019.05.113

Wang, C., Li, W., Wang, Y., Yang, X., Xu, S., 2020. Study of electrochemical corrosion on Q235A steel under stray current excitation using combined analysis by electrochemical impedance spectroscopy and artificial neural network. Constr. Build. Mater. 247, 118562. https://doi.org/10.1016/J.CONBUILDMAT.2020.118562

Wang, C., Li, W., Xin, G., Wang, Y., Xu, S., 2019b. Prediction Model of Corrosion Current Density Induced by Stray Current Based on QPSO-Driven Neural Network. Complexity 2019. https://doi.org/10.1155/2019/3429816

Wang, H., Yajima, A., Castaneda, H., 2019. A stochastic defect growth model for reliability assessment of corroded underground pipelines. Process Saf. Environ. Prot. 123, 179–189. https://doi.org/10.1016/J.PSEP.2019.01.005

Wang, J., Hu, J., Gu, C., Mou, Y., Yu, J., Zhong, X., 2022. The effect of pulse current cathodic protection on cathodic disbondment of epoxy coatings. Prog. Org. Coatings 170, 107001. https://doi.org/10.1016/J.PORGCOAT.2022.107001

Wang, Y., Zhang, P., Qin, G., 2019. Non-probabilistic time-dependent reliability analysis for suspended pipeline with corrosion defects based on interval model. Process Saf. Environ. Prot. 124, 290–298. https://doi.org/10.1016/J.PSEP.2019.02.028

Wang, Z., Shi, X., Yang, X.S., He, W., Shi, S.Q., Ma, X., 2021. Atomistic simulation of the effect of the dissolution and adsorption of hydrogen atoms on the fracture of α-Fe single crystal under tensile load. Int. J. Hydrogen Energy 46, 1347–1361. https://doi.org/10.1016/j.ijhydene.2020.09.216

Wasim, M., Shoaib, S., Mubarak, N.M., Inamuddin, Asiri, A.M., 2018. Factors influencing corrosion of metal pipes in soils. Environ. Chem. Lett. 2018 163 16, 861–879. https://doi.org/10.1007/S10311-018-0731-X

Xu, L.Y., Cheng, Y.F., 2013. Development of a finite element model for simulation and prediction of mechanoelectrochemical effect of pipeline corrosion. Corros. Sci. 73, 150–160. https://doi.org/10.1016/J.CORSCI.2013.04.004

Xu, L.Y., Cheng, Y.F., 2012. An experimental investigation of corrosion of X100 pipeline steel under uniaxial elastic stress in a near-neutral pH solution. Corros. Sci. 59, 103–109. https://doi.org/10.1016/J.CORSCI.2012.02.022

Xu, M., Lam, C.N.C., Wong, D., Asselin, E., 2020. Evaluation of the cathodic disbondment resistance of pipeline coatings – A review. Prog. Org. Coatings 146, 105728. https://doi.org/10.1016/J.PORGCOAT.2020.105728

Yan, M., Sun, C., Xu, J., Wu, T., Yang, S., Ke, W., 2015. Stress corrosion of pipeline steel under occluded coating disbondment in a red soil environment. Corros. Sci. 93, 27–38. https://doi.org/10.1016/J.CORSCI.2015.01.001

Yang, Y., Cheng, Y.F., 2016. Stress enhanced corrosion at the tip of near-neutral pH stress corrosion cracks on pipelines. Corrosion 72, 1035–1043. https://doi.org/10.5006/2045

Yanqiang, L., Wan, L., Hu, L., Zhou, S., Xiaoyang, Z., 2017. CN. Patent no. CN206706213U A kind of shallow embedding and the anodic protection flexible anode of deep well anode bed.

Yeom, K.J., Kim, W.S., Oh, K.H., 2016. Integrity assessment of API X70 pipe with corroded girth and seam welds via numerical simulation and burst test experiments. Eng. Fail. Anal. 70, 375–386. https://doi.org/10.1016/J.ENGFAILANAL.2016.09.008

Yuan, W., Huang, F., Liu, J., Hu, Q., Cheng, Y.F., 2018. Effects of temperature and applied strain on corrosion of X80 pipeline steel in chloride solutions. Corros. Eng. Sci. Technol. 53, 393–402. https://doi.org/10.1080/1478422X.2018.1491111

Zhang, P., Laleh, M., Hughes, A.E., Marceau, R.K.W., Hilditch, T., Tan, M.Y., 2023. A systematic study on the influence of electrochemical charging conditions on the hydrogen embrittlement behaviour of a pipeline steel. Int. J. Hydrogen Energy. https://doi.org/10.1016/J.IJHYDENE.2023.01.149

Zhang, T., Zhao, W., Li, T., Zhao, Y., Deng, Q., Wang, Y., 2018. Comparison of hydrogen embrittlement susceptibility of three cathodic protected subsea pipeline steels from a point of view of hydrogen permeation. Corros. Sci. 104–115. https://doi.org/10.1016/j.corsci.2017.11.013

Zhou, D., Li, T., Huang, D., Wu, Y., Huang, Z., Xiao, W., Wang, Q., Wang, X., 2021. The experiment study to assess the impact of hydrogen blended natural gas on the tensile properties and damage mechanism of X80 pipeline steel. Int. J. Hydrogen Energy 46, 7402–7414. https://doi.org/10.1016/j.ijhydene.2020.11.267

Zub, A.T., 2023. Strategic management: a textbook and a workshop for universities, 4th ed. Yurayt Publishing House, Moscow.

8. List of Figures

9. List of Tables

10. List of Abbreviations

AC	Alternating current
AIDE	Adsorption-Induced Dislocation Emission
CP	Cathodic protection
CPS	Cathodic protection station
DC	Direct current
ECC	Electrochemical corrosion
HE	Hydrogen embrittlement
HEDE	Hydrogen Enhanced Decohesion
HELP	Hydrogen-Enhanced Local Plasticity
HESIV	Hydrogen Enhanced Strain Induced Vacancy
HIC	Hydrogen induced cracking
SCC	Stress corrosion cracking
SWOT	Strengths, weaknesses, opportunities, threats

Annex Table of Contents

Annex

№ of the experiment		1	2	3	4	5	6
№	I, A	φ, V					
1	0	1.232	1.2319	1.232	1.2321	1.2321	1.2324
2	1	1.4171	1.4172	1.4171	1.471	1.4171	1.4177
3	2	1.6322	1.64	1.6321	1.631	1.631	1.6319
4	3	1.8853	1.883	1.8826	1.8841	1.8828	1.8833
5	4	2.1031	2.1025	2.1021	2.1022	2.1028	2.102
6	5	2.3037	2.3038	2.3036	2.3035	2.3039	2.314
7	6	2.4999	2.5	2.4999	2.4998	2.5002	2.5002
8	7	2.6599	2.6601	2.6596	2.6597	2.6596	2.6597
9	8	2.897	2.908	2.903	2.902	2.898	2.908
10	9	3.1801	3.185	3.1843	3.187	3.1865	3.1815
11	10	3.3122	3.3167	3.3123	3.3125	3.312	3.3122
12	11	3.5473	3.5472	3.5473	3.5489	3.5471	3.547
13	12	3.7524	3.7524	3.7527	3.7522	3.7524	3.7589
14	13	3.9425	3.9424	3.9426	3.9426	3.9422	3.9421

Annex table 1: Current strength and protective potential difference values at the drainage point for the 6 experiments at the 360 km CPS

№ of the experiment		1	2	3	4	5	6
№	I, A	φ, V					
1	0	1.191	1.192	1.193	1.193	1.191	1.191
2	3	1.198	1.197	1.197	1.198	1.187	1.199
3	6	1.207	1.2	1.205	1.201	1.201	1.207
4	9	1.218	1.215	1.215	1.208	1.214	1.218
5	12	1.228	1.227	1.226	1.228	1.226	1.228
6	15	1.234	1.235	1.238	1.246	1.234	1.239
7	18	1.247	1.247	1.249	1.25	1.247	1.248
8	21	1.256	1.253	1.252	1.254	1.253	1.253

Annex table 2: Current strength and protective potential difference values at the drainage point for the 6 experiments at the 336 km CPS

№ of the experiment		1	2	3	4	5	6
№	I, A	φ, V					
1	0	1.71	1.7105	1.71	1.71	1.71	1.7102
2	3	1.741	1.7414	1.742	1.741	1.741	1.7414
3	6	1.772	1.772	1.781	1.762	1.7814	1.7815
4	9	1.809	1.8	1.802	1.7892	1.81	1.798
5	12	1.843	1.8428	1.843	1.843	1.85	1.831
6	15	1.881	1.8819	1.88	1.898	1.889	1.871
7	18	1.921	1.956	1.949	1.951	1.951	1.945
8	21	1.962	1.958	1.961	1.96	1.96	1.951

Annex table 3: Current strength and protective potential difference values at the drainage point for the 6 experiments at the 345 km CPS

№ of the experiment		1	2	3	4	5	6
№	I, A	φ, V					
1	0	1.393	1.393	1.391	1.392	1.394	1.392
2	3	1.398	1.397	1.399	1.397	1.398	1.399
3	6	1.407	1.411	1.412	1.41	1.413	1.41
4	9	1.423	1.423	1.425	1.424	1.424	1.426
5	12	1.434	1.435	1.436	1.436	1.434	1.435
6	15	1.442	1.451	1.45	1.45	1.45	1.451
7	18	1.462	1.463	1.462	1.46	1.464	1.461
8	21	1.475	1.473	1.475	1.472	1.476	1.476

Annex table 4: Current strength and protective potential difference values at the drainage point for the 6 experiments at the 371 km CPS

№ of the experiment		1	2	3	4	5	6
№	I, A	φ, V					
1	0	1.522	1.521	1.521	1.52	1.523	1.521
2	3	1.533	1.533	1.533	1.532	1.533	1.534
3	6	1.546	1.541	1.544	1.539	1.54	1.543
4	9	1.564	1.557	1.531	1.562	1.561	1.564
5	12	1.583	1.58	1.577	1.58	1.583	1.579
6	15	1.587	1.592	1.591	1.593	1.593	1.592
7	18	1.598	1.605	1.602	1.61	1.603	1.601
8	21	1.611	1.611	1.608	1.609	1.608	1.606

Annex table 5: Current strength and protective potential difference values at the drainage point for the 6 experiments at the 384 km CPS